

CASE 1111
COPY

NASA TECHNICAL NOTE



NASA TN D-3848

NASA TN D-3848

A THREE-DIMENSIONAL ANALYSIS OF
A TANGENTIAL YO-YO DESPIN DEVICE
ON A ROTATING BODY

by Robert L. Collins, Jr.

Langley Research Center

Langley Station, Hampton, Va.

NATIONAL AERONAUTICS AND SPACE ADMINISTRATION • WASHINGTON, D. C. • MARCH 1967

A THREE-DIMENSIONAL ANALYSIS OF A TANGENTIAL YO-YO
DESPIN DEVICE ON A ROTATING BODY

By Robert L. Collins, Jr.

Langley Research Center
Langley Station, Hampton, Va.

NATIONAL AERONAUTICS AND SPACE ADMINISTRATION

For sale by the Clearinghouse for Federal Scientific and Technical Information
Springfield, Virginia 22151 - CFSTI price \$3.00

A THREE-DIMENSIONAL ANALYSIS OF A TANGENTIAL YO-YO DESPIN DEVICE ON A ROTATING BODY

By Robert L. Collins, Jr.
Langley Research Center

SUMMARY

The problem of despinning a rotating rigid body by the release of yo-yo despin weights is considered. Although studies have been made previously for the two-dimensional case of a fixed spin axis, there has been little effort to incorporate an initial coning angle which, in general, leads to a three-dimensional problem. This study considers the effect of an initial coning motion on the parameters which influence the design of a yo-yo despin system. The differential equations of motion of the system are derived for a symmetric rigid body and these are integrated numerically to provide solutions for several specific cases. The results show that a two-dimensional study is sufficient to predict such parameters as cable length, cable tension, and time required to despin, as long as the initial coning angle is less than 10° to 30° , and the masses of the despin weights are not too small. The parameters plotted in this study give an indication of the effects of initial coning angle on the design parameters of interest for what is called tangential motion.

INTRODUCTION

A typical problem area in the design of earth orbiting satellites is the reduction of the angular velocity which may occur after injection into orbit. One efficient technique of despinning a satellite is by the use of a so-called yo-yo despin device. Basically, this device is a simple arrangement of small masses attached to cables which are wound about the periphery of the spinning body in a plane perpendicular to the spin axis. When it is desired to reduce the rotational rate of the body, the despin weights are released and they move away from the body constrained only by the cables which unwrap from the body. The tension produced in the cables causes a moment which reduces the spin rate of the body. Essentially, the angular rotation of the body is reduced by transferring a desired quantity of angular momentum from the body to the despin weights. When sufficient angular momentum is transferred to obtain the desired reduced body spin rate, the cables are released from the body which then rotates in space independent of the yo-yo system.

In this study it is assumed that the cables are initially wrapped in a circle about the body and therefore, during the unwinding phase of the motion, the cables will remain tangent to this "wrapping circle." This phase of the motion has been referred to as "Phase I" motion in reference 2; however, the terminology "tangential phase motion" is used in this paper. Many previous two-dimensional studies have also included a second phase to the motion in which the cables are assumed to have a fixed length and are attached to the body by a hinge at the end opposite the despin weights. Once the cables have unwrapped to their full length they swing away from the tangent until they are at some specified angle with the tangent, usually 90° , and then they are released. This phase of the motion has been referred to as "Phase II" motion. This paper does not consider despin cases which include this "nontangential" or Phase II motion.

A particularly simple analysis of the motion of the yo-yo system may be made when there is no initial coning motion of the system. This motion is possible if the initial angular rotation vector of the system lies along the axis of symmetry. In this case the initial angular momentum also lies along the spin axis and if there are no disturbances on the despin weights or the body, the weights will move away from the body in a plane always perpendicular to the symmetry axis. The angular momentum vector, the angular rotation vector, and the axis of symmetry will then remain in a fixed direction in space and the resulting analysis can be treated as two dimensional. Thus, the two-dimensional motion requires that the movement of the despin weights and cables take place in a plane fixed in space and containing the initial circle of winding.

A study of the tangential phase of the two-dimensional motion yields exact analytical expressions for the variables of interest. The equations of motion for the fixed or nontangential phase in the two-dimensional case have not been solved as in the tangential phase but some results can be obtained through the conservation of energy and angular momentum principles. Studies of this type are presented in references 1 to 4. Reference 2 gives a very concise treatment and also discusses the correction necessary to account, approximately, for the mass of the cables. Further studies of the two-dimensional yo-yo are found in reference 5 where it is noted that variations from the nominal design conditions may be partially nullified by using elastic cables. An analysis of this "stretch yo-yo" and some experimental data are found in references 6 and 7.

An approximate solution for a three-dimensional problem is found in reference 8, but so many approximations are made on the configuration and kinematics of the system that it is not applicable for general studies of yo-yo despin systems. Reference 11, however, gives a comprehensive study of the three-dimensional problem considering both phases of the motion but does not give results for complete despin by tangential phase motion only.

This paper presents a three-dimensional analysis of the parameters of motion which are of interest in the design and study of a yo-yo despin system. The assumptions made on the system are similar to those of the two-dimensional tangential phase studies with certain additional hypotheses which keep this analysis from becoming too complex. The equations of motion for the system are written by applying the Euler equations for rigid body motion to the rigid body and Newton's second law to a despin weight. This technique was used since it is directly applicable to this system while the Lagrangian or the Hamiltonian techniques require special attention and cannot be directly applied by the usual methods. The Lagrangian methods are invalid, in their usual formulation, for this problem because certain assumptions have been made about the configuration of the system which introduces constraining forces that do work during a virtual displacement of the generalized coordinates. This procedure is contrary to the basic postulates of analytical mechanics and therefore the equations usually derived from this approach cannot be used without modification. In this vein it is also of interest to note that for the system studied herein, the total system kinetic energy decreases throughout the motion whenever the despin cables and weights are out of the initial plane of their winding. This decrease may be verified by making a detailed examination of the results presented and computing the system kinetic energy at several instants during the motion. Further discussion of this system may be found in reference 11.

The equations of motion were integrated on digital computer and the solutions were checked by three separate means. First, the results for the two-dimensional theory previously mentioned agree with these solutions for the two-dimensional cases; second, the components of the system angular momentum vector were checked in fixed space and were found to remain constant, and third, an expression for the sum of the time rate of change of the system kinetic energy and the time rate of change of the work done by the system was found to be essentially zero as it should be. These checks are very conclusive as to the validity of the results presented.

SYMBOLS

a	radius of cable windings
$\hat{\mathbf{A}}$	acceleration vector of despin weight
\tilde{A}	nondimensional magnitude of acceleration of despin weight
$\tilde{A}_1, \tilde{A}_2, \tilde{A}_3$	components of acceleration vector $\hat{\mathbf{A}}$ along x_1 , x_2 , and x_3 axes
a_{ij}	elements of matrix from equations of motion (eq. (9))

\tilde{a}_{ij}	nondimensional form of elements a_{ij} (eq. (12))
$\tilde{\tilde{a}}_{ij}$	elements of inverse matrix of \tilde{a}_{ij}
b_1, b_2, b_3	auxiliary symbol for terms in equations of motion (eq. (9))
$\tilde{b}_1, \tilde{b}_2, \tilde{b}_3$	nondimensional form of b_1, b_2, b_3 (eq. (12))
C_1, C_2, C_3	Coriolis and centrifugal acceleration terms (eq. (A13))
C	conversion factor (eq. (19))
E_1, E_2, E_3	Euler acceleration terms (eq. (A14))
i, j	indices
$\hat{i}, \hat{j}, \hat{k}$	unit vectors along x_1, x_2 , and x_3 axes
I	inertia ratio of body, I_3/I_1
I_1, I_2, I_3	mass moments of inertia about x_1, x_2 , and x_3 axes
K	inertia factor for despin weights, $\frac{2ma^2}{I_1}$
l	length of cable unwound
m	mass of a single despin weight
\hat{M}	moment vector acting on body
m_b	mass of body without weights
r	distance from mass center to despin weight
t	time
T	tension in cable
\hat{T}	vector tension acting on body, directed toward weight

\tilde{T}	nondimensional tension in cable
$\hat{\tilde{V}}$	nondimensional velocity of despin weight
$\tilde{V}_1, \tilde{V}_2, \tilde{V}_3$	components of velocity of despin weight along x_1 , x_2 , and x_3 axes (eq. (A7))
x_j	quantities representing $\ddot{\beta}$, $\ddot{\alpha}$, and T
x_1, x_2, x_3	coordinate axes with origin fixed at mass center, directed along principal axes of body
y_1, y_2, \dots, y_7	variables introduced to reduce second-order equations (eq. (14))
α	cable out-of-plane angle (sketch (1))
β	unwind angle (sketch (1))
Γ	coning angle (between \hat{k} and angular momentum vector)
δ	spinning angle (between \hat{k} and $\hat{\omega}$)
$\hat{\tilde{r}}$	nondimensional radius vector \hat{r}/a from mass center to despin weight
$\tilde{r}_1, \tilde{r}_2, \tilde{r}_3$	components of $\hat{\tilde{r}}$ along x_1 , x_2 , and x_3 axes
$\tilde{r}_{1\beta}, \tilde{r}_{2\beta}, \tilde{r}_{3\beta}$	partial derivatives of $\tilde{r}_1, \tilde{r}_2, \tilde{r}_3$ with respect to β
$\tilde{r}_{1\alpha}, \tilde{r}_{2\alpha}, \tilde{r}_{3\alpha}$	partial derivatives of $\tilde{r}_1, \tilde{r}_2, \tilde{r}_3$ with respect to α
τ	nondimensional time
$\hat{\omega}$	angular velocity vector
$\hat{\tilde{\omega}}$	nondimensional angular velocity vector
$\hat{\tilde{\omega}}^*$	nondimensional angular velocity vector (eq. (A6))
$\omega_1, \omega_2, \omega_3$	components of angular velocity along x_1 , x_2 , and x_3 axes

$\tilde{\omega}_1, \tilde{\omega}_2, \tilde{\omega}_3$ nondimensional form of $\omega_1, \omega_2, \omega_3$

$\tilde{\omega}_{12}$ nondimensional cross-axis spin rate, $\sqrt{\omega_1^2 + \omega_2^2}$

Dots over symbols indicate time derivatives; primes denote dimensionless time derivatives. A caret $\hat{}$ over a symbol denotes a vector quantity and a tilde \sim over a symbol denotes nondimensionalization. Quantities subscripted with 0 indicate that the initial time ($t = t_0$) is being referred to.

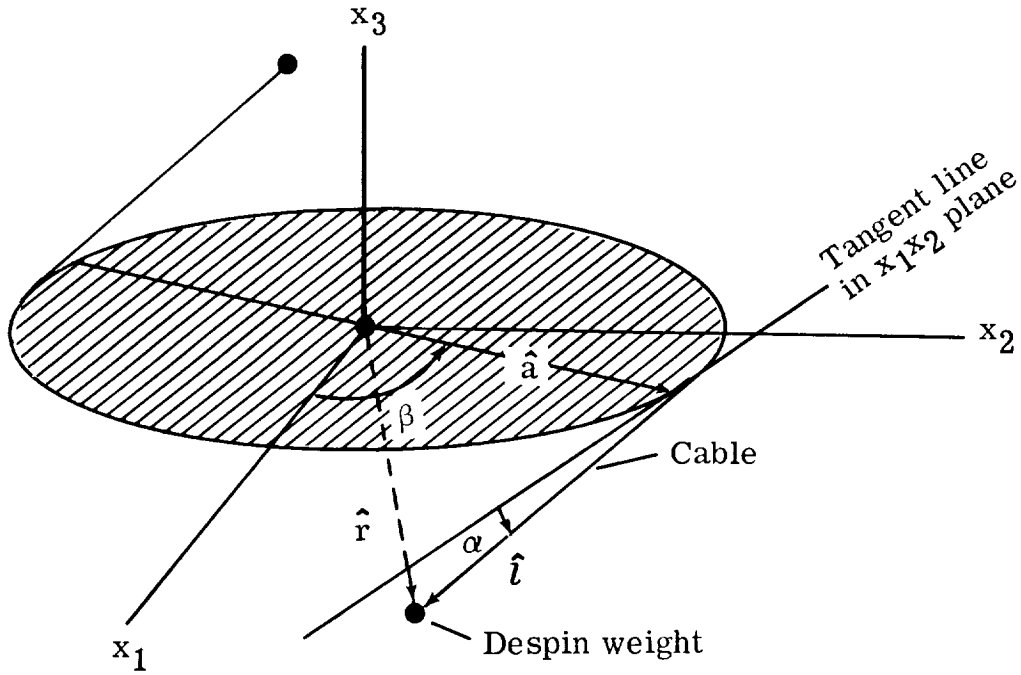
ANALYSIS

Derivation of Equations of Motion

The despin system which is analyzed in this report consists of a symmetric rigid body and two small masses or despin weights as they will be called. Each mass is coupled to the rigid body by a perfectly flexible, inextensible, and massless cable which is initially wound about the body. These cables are wrapped so that the despin weights are diametrically opposite each other through the mass center of the rigid body at the initial instant. The cables are assumed to be wrapped on the periphery of a circle which has its center at the mass center of the rigid body and is perpendicular to the symmetry axis of the rigid body. When the despin weights are released, they move outward and are constrained only by the cables which connect them to the body. The force of constraint acting on a weight is the tension in the cable and this tension manifests itself in a torque which tends to retard the spin of the rigid body. Therefore, there is a strong interaction or coupling between the motion of the rigid body and that of the weights.

The body-axes coordinate system and some of the quantities used to describe the system configuration are found in sketch (1). A right-handed orthogonal coordinate system x_1, x_2, x_3 is fixed in the rigid body with its origin at the mass center of the body, and the x_3 -axis lying along the symmetry axis of the body. Because of the symmetry of the body, any choice of orientation of the x_1, x_2 axes produces a set of principal axes. The choice for the x_1 -axis, however, will be made so that it is aligned with a despin weight when that weight and cable arrangement is completely wound on the winding circle. The second despin weight then lies initially along the negative x_1 -axis. The x_2 -axis completes the right-handed triad.

Since the despin weights are initially released with positions and velocities symmetric through the origin, they will remain symmetric through the origin throughout the motion. Because of this symmetry it will be necessary to analyze only one despin weight and the weight initially along the positive x_1 -axis is used.



Sketch (1)

The position of this weight is specified in terms of the body-axis coordinate system. As the cable unwinds, the point of contact where the cable leaves the body is defined by the vector \hat{a} which is rotated an angle β from the x_1 -axis. The unwound cable is represented by the vector \hat{l} in sketch (1) and must lie in a plane tangent to the cable winding circle and parallel to the x_3 -axis. The angle α is the angular measure of the vector \hat{l} from the plane of the x_1, x_2 axes. It should be noted that, as defined here, a positive α corresponds to the despin weight being "below" the x_1, x_2 plane in the sense of positive x_3 being "above" this plane. The angle β is referred to as the unwind angle and α as the out-of-plane angle.

The length of cable unwound is given by the relation

$$l = a\beta \quad (1)$$

where a is the radius of the cable winding circle and where l is the magnitude of the vector \hat{l} . With the constraint relation (1), the position vector \hat{r} may be written with components along the body-axis coordinate system entirely in terms of the angles α and β . These components are seen from the geometry of sketch (1) to be

$$\left. \begin{aligned} r_1 &= a(\cos \beta + \beta \sin \beta \cos \alpha) \\ r_2 &= a(\sin \beta - \beta \cos \beta \cos \alpha) \\ r_3 &= -a\beta \sin \alpha \end{aligned} \right\} \quad (2)$$

Because of the symmetry of the system, the mass center of the rigid body and the mass center of the system occupy the same position in inertial space. Therefore, the motion of the body is essentially that of a symmetric rigid body rotating about a fixed point at the mass center and being acted upon by a moment which is varying with time. This moment is due to the cable tension which acts along the vector \hat{l} . The angular velocity vector $\hat{\omega}$ of the body is denoted by the components ω_1 , ω_2 , and ω_3 along the body axes. The force acting on the body due to the tension T in the cable is denoted by the vector \hat{T} and the moment due to this tension is \hat{M} . This moment is generated by the two cables and may be expressed as

$$\hat{M} = 2\hat{a} \times \hat{T}$$

The force vector due to the tension \hat{T} and the vector \hat{a} are seen from the geometry of sketch (1) to be

$$\hat{T} = T(\sin \beta \cos \alpha \hat{i} - \cos \beta \cos \alpha \hat{j} - \sin \alpha \hat{k}) \quad (3)$$

$$\hat{a} = a(\cos \beta \hat{i} + \sin \beta \hat{j}) \quad (4)$$

Where \hat{i} , \hat{j} , and \hat{k} are the usual unit vectors along the x_1 , x_2 , and x_3 body axes, respectively. The moment vector then becomes

$$\hat{M} = -2aT(\sin \alpha \sin \beta \hat{i} - \sin \alpha \cos \beta \hat{j} + \cos \alpha \hat{k}) \quad (5)$$

The equations of motion of the body are obtained directly by use of the Euler equations for rigid body motion about a fixed point. These equations may be found in reference 10, and for this symmetric rigid body become

$$\left. \begin{aligned} I_1 \dot{\omega}_1 - (I_1 - I_3) \omega_2 \omega_3 &= -2aT \sin \alpha \sin \beta \\ I_1 \dot{\omega}_2 - (I_3 - I_1) \omega_1 \omega_3 &= 2aT \sin \alpha \cos \beta \\ I_3 \dot{\omega}_3 &= -2aT \cos \alpha \end{aligned} \right\} \quad (6)$$

where I_2 is replaced by its equivalent value I_1 due to symmetry.

Equations (6) are three differential equations for six unknown quantities ω_1 , ω_2 , ω_3 , α , β , and T . Therefore, it is necessary to obtain three other expressions in order to specify the system completely. These expressions are obtained by applying Newton's second law to a single despin weight.

The despin weight specified by the vector \hat{r} , which has components along x_1 , x_2 , and x_3 given by equations (2), has a force acting on it caused by the cable tension represented by $-\hat{T}$. Therefore,

$$-\hat{T} = m \frac{d^2 \hat{r}}{dt^2} \quad (7)$$

In this report the notation d/dt , d^2/dt^2 refers to derivatives with respect to time in an inertial sense and $(\dot{})$, $(\ddot{})$ refers to derivatives taken in the x_1, x_2, x_3 body-axis system. With this definition the absolute velocity and acceleration vector components along the body axes become

$$\left. \begin{aligned} \frac{d\hat{r}}{dt} &= \dot{\hat{r}} + \hat{\omega} \times \hat{r} \\ \frac{d^2\hat{r}}{dt^2} &= \ddot{\hat{r}} + \dot{\hat{\omega}} \times \hat{r} + 2\hat{\omega} \times \dot{\hat{r}} + \hat{\omega} \times (\hat{\omega} \times \hat{r}) \end{aligned} \right\} \quad (8)$$

Equations (2), (3), (7), and (8) may be manipulated to provide three second-order differential equations involving the quantities ω_1 , ω_2 , ω_3 , α , β , and T and their derivatives. These equations will be independent of the three equations derived for the rigid body (eqs. (6)) and therefore a complete set of six differential equations and six unknowns is established.

The manipulations and differentiations required to obtain the desired relations are given in appendix A where it is shown that equation (7) may be written in the form

$$\sum_{j=1}^3 a_{ij} X_j = b_i \quad (i = 1, 2, \text{ and } 3) \quad (9)$$

The notation X_j which will be used again, signifies that the components of X_j are the quantities $\ddot{\beta}$, $\ddot{\alpha}$, and T in that order for $j = 1, 2, 3$, and where the coefficients a_{ij} are given functions of α and β only and the components b_i are functions of ω_1 , ω_2 , ω_3 , α , β , $\dot{\alpha}$, and $\dot{\beta}$.

Equations (6) and (9) are the governing equations for this system, which can be integrated to yield ω_1 , ω_2 , ω_3 , α , β , and T . These equations are nonlinear and it is very doubtful that an exact closed form solution can be obtained; therefore, integration of the equations by some numerical procedure is necessary.

Nondimensionalization

In this section the parameters which appear in equations (6) and (9) are put into a convenient nondimensional form for computation and for presentation of the results. It may be noted that equations (6) and (9) as they stand contain the variables ω_1 , ω_2 , ω_3 , α , β , T , and t and constants I_1 , I_3 , m , a and that after nondimensionalizing, the variables are $\tilde{\omega}_1$, $\tilde{\omega}_2$, $\tilde{\omega}_3$, $\tilde{\alpha}$, $\tilde{\beta}$, \tilde{T} , and τ whereas the constants are I and K . Note that the number of variables is the same and the constants are reduced to two.

When nondimensionalized in the manner presented herein, the variables become independent of the constants I and K for the tangential two-dimensional case. This form then has the advantage that one curve, in the family of curves to be presented, corresponding to the two-dimensional or zero coning case will be the same for any of the values of the I and K which are to be chosen for study. This choice of nondimensionalization therefore results in more convenient and uniform plots. For these reasons, the following nondimensional quantities are defined.

$$\left. \begin{aligned} I &= \frac{I_3}{I_1} \\ K &= \frac{2ma^2}{I_1} \\ \tilde{\omega}_1 &= \frac{\omega_1}{\omega_{30}} \\ \tilde{\omega}_2 &= \frac{\omega_2}{\omega_{30}} \\ \tilde{\omega}_3 &= \frac{\omega_3}{\omega_{30}} \\ \tilde{\beta} &= \frac{\beta}{\sqrt{1 + \frac{I}{K}}} \\ \tilde{\alpha} &= \frac{\alpha}{\sqrt{1 + \frac{I}{K}}} \\ \tilde{T} &= \sqrt{1 + \frac{I}{K}} \frac{2aT}{I_3 \omega_{30}} \\ \tau &= \frac{\omega_{30}}{\sqrt{1 + \frac{I}{K}}} t \end{aligned} \right\} \quad (10)$$

Note that

$$\frac{I}{K} = \frac{I_3}{2ma^2}$$

The subscript o in ω_{30} implies that the angular velocity at the initial time is being considered.

The equations of motion can then be rewritten in terms of these new parameters. If the derivatives with respect to the nondimensional time τ are denoted by primes, equations (6) become

$$\left. \begin{aligned} \tilde{\omega}'_1 &= (1 - I)\sqrt{1 + \frac{I}{K}} \tilde{\omega}_2 \tilde{\omega}_3 - I\tilde{T} \sin \alpha \sin \beta \\ \tilde{\omega}'_2 &= (I - 1)\sqrt{1 + \frac{I}{K}} \tilde{\omega}_1 \tilde{\omega}_3 + I\tilde{T} \sin \alpha \cos \beta \\ \tilde{\omega}'_3 &= -\tilde{T} \cos \alpha \end{aligned} \right\} \quad (11)$$

where α and β are

$$\alpha = \tilde{\alpha} \sqrt{1 + \frac{I}{K}}$$

$$\beta = \tilde{\beta} \sqrt{1 + \frac{I}{K}}$$

equations (9) rewritten in terms of these nondimensional parameters become

$$\sum_{j=1}^3 \tilde{a}_{ij} \tilde{X}_j = \tilde{b}_i \quad (i = 1, 2, \text{ and } 3) \quad (12)$$

where again \tilde{X}_j corresponds to quantities $\tilde{\beta}'$, $\tilde{\alpha}'$, and \tilde{T} and where \tilde{a}_{ij} and \tilde{b}_i are functionally

$$\tilde{a}_{ij} = \tilde{a}_{ij}(I, K; \tilde{\alpha}, \tilde{\beta})$$

$$\tilde{b}_i = \tilde{b}_i(I, K; \tilde{\omega}_1, \tilde{\omega}_2, \tilde{\omega}_3, \tilde{\alpha}', \tilde{\beta}', \tilde{\alpha}, \tilde{\beta})$$

The complete expressions for the \tilde{a}_{ij} and \tilde{b}_i are found in appendix A along with a derivation of the equations and their nondimensionalization. Equations (11) and (12) are the equations of motion which will provide the information to be presented in this report.

Integration of Equations of Motion

Equations (12) are not directly amenable to the usual techniques of integration by digital computer since the left-hand side is a linear combination of the variable \tilde{T} and of the second derivatives of $\tilde{\alpha}$ and $\tilde{\beta}$. Therefore, in order to put these equations into a more fundamental form, the components \tilde{X}_j are solved by use of Cramer's rule so that

$$\tilde{X}_i = \sum_{j=1}^3 \tilde{a}_{ij} \tilde{b}_j \quad (i = 1, 2, \text{ and } 3) \quad (13)$$

where the $\tilde{\tilde{a}}_{ij}$ are the elements of a matrix which is the inverse of the matrix with elements \tilde{a}_{ij} .

Equations (13) provide explicit relationships for the derivatives \tilde{a}' and $\tilde{\beta}'$ and also for the variable \tilde{T} . In order to obtain a complete set of first-order differential equations in place of equations (11) and (13), a new set of variables are defined as follows:

$$\left. \begin{aligned} y_1 &= \tilde{\omega}_1 \\ y_2 &= \tilde{\omega}_2 \\ y_3 &= \tilde{\omega}_3 \\ y_4 &= \tilde{\beta} \\ y_5 &= \tilde{\alpha} \\ y_6 &= \tilde{\beta}' \\ y_7 &= \tilde{\alpha}' \end{aligned} \right\} \quad (14)$$

With these new variables, equations (11) and (13) may be written as a set of algebraic and first-order differential equations:

$$\left. \begin{aligned} \tilde{T} &= \sum_{i=1}^3 \tilde{\tilde{a}}_{3i} \tilde{b}_i \\ y_1' &= \sqrt{1 + \frac{I}{K}} (1 - I) y_2 y_3 - I \tilde{T} \sin \sqrt{1 + \frac{I}{K}} \tilde{\alpha} \sin \sqrt{1 + \frac{I}{K}} \tilde{\beta} \\ y_2' &= \sqrt{1 + \frac{I}{K}} (I - 1) y_1 y_3 + I \tilde{T} \sin \sqrt{1 + \frac{I}{K}} \tilde{\alpha} \cos \sqrt{1 + \frac{I}{K}} \tilde{\beta} \\ y_3' &= -\tilde{T} \cos \sqrt{1 + \frac{I}{K}} \tilde{\alpha} \\ y_4' &= y_6 \\ y_5' &= y_7 \\ y_6' &= \sum_{i=1}^3 \tilde{\tilde{a}}_{1i} \tilde{b}_i \\ y_7' &= \sum_{i=1}^3 \tilde{\tilde{a}}_{2i} \tilde{b}_i \end{aligned} \right\} \quad (15)$$

Equations (15) are now in a convenient form for numerical integration. However, at the initial instant the coefficient matrix of equations (12) is singular. Hence, special methods must be used to begin the integration and a simple technique is shown in appendix B which overcomes this difficulty. The only initial quantities needed to begin the integration are the constants I and K and the variables $\tilde{\omega}_{10}$ and $\tilde{\omega}_{20}$. All other variables are obtained by setting the unwind angle β and the relative velocity \hat{r} equal to zero at the initial instant. This result is also shown in appendix B.

Descriptive Parameters of the Motion

Thus far, it has been shown that the motion of the tangential yo-yo despin system analyzed in this report can be described in terms of the quantities $\tilde{\omega}_1$, $\tilde{\omega}_2$, $\tilde{\omega}_3$, $\tilde{\alpha}$, $\tilde{\beta}$, the nondimensional tension \tilde{T} , and the nondimensional time τ . A particular motion results from a choice of the quantities I and K and the initial conditions $\tilde{\omega}_{10}$ and $\tilde{\omega}_{20}$. Two other quantities which are of interest are the initial coning angle Γ_0 and the cross-axis spin rate $\tilde{\omega}_{12}$. The initial coning angle is the angle between the angular momentum vector and the axis of symmetry of the system before the despin process takes place. The motion before deployment of the despin weights is characterized by this coning angle and is described in references 8 and 9.

Since both the axis of symmetry and the angular momentum vector of the rigid body move in inertial space during the despin process, the instantaneous value of the coning angle is somewhat academic, but the initial value Γ_0 is important in the physical interpretation it provides. The coning angle is computed from

$$\Gamma = \tan^{-1} \left(\frac{\tilde{\omega}_{12}}{I\tilde{\omega}_3} \right) \quad (16)$$

where $\tilde{\omega}_{12}$ is the cross-axis spin rate and is the magnitude of the nondimensional angular rotation vector in the x_1, x_2 plane or

$$\tilde{\omega}_{12} = \sqrt{(\tilde{\omega}_1)^2 + (\tilde{\omega}_2)^2} \quad (17)$$

Another angle which has some academic importance and which is presented in the data is the spinning angle δ . This angle is the angle between the angular rotation vector and the body symmetry axis or

$$\delta = \tan^{-1} \left(\frac{\tilde{\omega}_{12}}{\tilde{\omega}_3} \right) \quad (18)$$

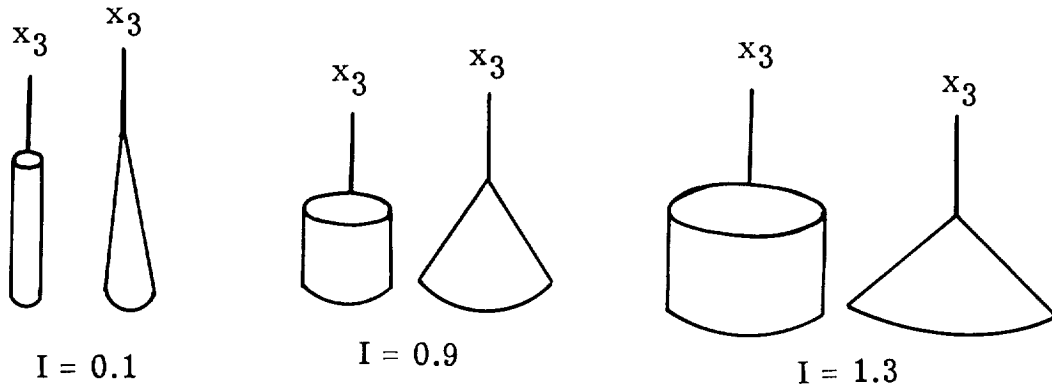
From the relations (16) and (17) it may be seen that the initial values $\tilde{\omega}_{10}$ and $\tilde{\omega}_{20}$ may be determined from Γ_0 and $\tilde{\omega}_{20}/\tilde{\omega}_{10}$. In the subsequent analysis these latter

quantities are used as initial conditions rather than $\tilde{\omega}_{10}$ and $\tilde{\omega}_{20}$. Appendix B gives the relations necessary to obtain $\tilde{\omega}_{10}$ and $\tilde{\omega}_{20}$ from Γ_0 and $\tilde{\omega}_{10}/\tilde{\omega}_{20}$.

RESULTS AND DISCUSSION

The equations of motion can be integrated once the constants I and K and the initial conditions ω_{20}/ω_{10} and Γ_0 are specified. The integrations are ended when the symmetry axis spin rate ω_3 is reduced to zero or if some other condition which is physically unrealistic occurs. For instance, the integrations end whenever α becomes 90° , since this condition would most likely correspond to physical interference between the cable or despin weight and the rigid body. Another physical restriction on the variables occurs when the unwind angle β reaches a maximum value and begins to decrease. This "rewinding" of the cable (that is, β decreasing) is not physically possible since it requires a constraint at the point of contact of the cable and winding circle (defined by \hat{a}) to "tuck" the cable back into or along the winding circle. Since a mechanism to provide such a constraint is not considered in this study, the event of β decreasing is not allowed.

Three values of I were chosen for this investigation which would represent different geometrical configurations for a rigid body of constant density. Sketch (2) shows the relative geometry of right circular cylinders and cones which have the inertia ratios: $I = 0.1, 0.9$, and 1.3 used in this study.



Sketch (2)

The inertia ratio K is an important design parameter since it contains both the despin mass m and the initial cable winding radius a . In order to obtain realistic values for this parameter, the right circular cone and right circular cylinder were again considered. If a constant mass density is assumed, it is possible from the equations of mechanics to derive the following relationships:

$$K = 4 \left(\frac{m}{m_b} \right) I \quad (\text{Cylinder})$$

$$K = \frac{15}{4} \left(\frac{m}{m_b} \right) I \quad (\text{Cone})$$

where m_b is the mass of the rigid body and m is the mass of a single despin weight. Therefore, if I is known, the inertia ratio K is determined by the ratio m/m_b . In this paper the value of the mass ratio was chosen to lie between the limits of 0.0005 to 0.05 which correspond to a total mass for both despin weights of 0.1 percent to 10 percent of the body mass. The value of K from these considerations must be approximately

$$0.0002 \leq K \leq 0.02 \quad (I = 0.1)$$

$$0.0018 \leq K \leq 0.18 \quad (I = 0.9)$$

$$0.0026 \leq K \leq 0.26 \quad (I = 1.3)$$

The parameter ω_{20}/ω_{10} was taken as unity in every case of this study. This value was assumed to be a representative one and a change in this value should not affect the general trend of the results obtained here, especially for the smaller coning angles. Changing this ratio essentially varies the initial conditions $\tilde{\alpha}'_0$, $\tilde{\beta}'_0$, and \tilde{T}_0 .

The initial coning angles studied are $\Gamma_0 = 0^\circ, 10^\circ, 20^\circ, 30^\circ, 40^\circ$, and 50° . The angle of 50° seems to be a reasonable upper limit for practical considerations since at this value the body has a larger component of angular momentum in the x_1, x_2 plane than along the symmetry axis. It should be recalled that the initial condition $\Gamma_0 = 0^\circ$ implies that the ensuing motion is two dimensional.

Figures 1, 2, and 3 are time histories of the quantities $\tilde{\omega}_{12}$, $\tilde{\omega}_3$, \tilde{T} , Γ , δ , $\tilde{\alpha}$, and $\tilde{\beta}$ for various values of Γ_0 and for three specific sets of values for I and K . Figures 4, 5, and 6 are presented to give some indication of the effects of changes in the design quantity K on several important parameters of the motion for the three geometries specified by $I = 0.1, 0.9$, and 1.3 .

Time histories for a particular body despin weight system $I = 0.1$, $K = 0.001$ are presented in figure 1. The most significant features are the nearly constant values of the cross-axis spin and small effect of coning angle on the spin rate, cable tension, and cable length. The design quantities $\tilde{\omega}_3$, \tilde{T} , and $\tilde{\beta}$ could have been predicted very accurately by the two-dimensional techniques given in reference 2. In figure 1(d) the coning angle and spinning angles are presented. At despin ($\omega_3 = 0$), these angles are both 90° which will always be the case when some residual tumbling rate or residual cross axis spin rate exists. Figure 1(e) reveals that the maximum value of the out-of-plane angle is approximately two-thirds of the initial coning angle.

In figure 2, time histories are presented for the same parameters as in figure 1 but for the different geometrical case $I = 0.9$, $K = 0.01$. It is significant to note that there is considerable deviation from the two-dimensional case of all the variables plotted for initial coning angles of about 30° or larger. Also note that there is a decrease in the cross-axis spin rate $\tilde{\omega}_{12}$ during the despin which is usually desirable since the final value is the residual tumbling rate after despin. The out-of-plane angle (fig. 2(e)) has a maximum value which is approximately twice the initial coning angle.

It was mentioned previously that whenever the angle β reached a (local) maximum during the despin process and then began to decrease, the integration was stopped. This event occurs on the $\Gamma_0 = 50^\circ$ case of figure 2. Figure 2(f) shows β reaching its maximum where its slope is zero. At this point the integration is stopped and this occurrence is noted in figure 2(b) which shows that the symmetry axis spin rate has a value of about 0.075 at the end of the integration.

Figure 3 is a set of time histories of the significant parameters of the motion for $I = 1.3$ and $K = 0.015$. The trends of the variations are similar to those of figure 2; however, the magnitudes of the variations are considerably larger. The maximum values of the angle α are, as in the previous case, about twice the initial coning angle. The case of β reaching a maximum value does not occur in these cases, although, as indicated in figure 3(f), the slope of the curve of $\tilde{\beta}$ plotted against τ for $\Gamma_0 = 50^\circ$ and $\tau = 0.5$ is very nearly zero. When compared with the curves of figure 1, the variations of these curves from the two-dimensional case ($\Gamma_0 = 0^\circ$) are very large.

The figures showing the nondimensional cable tension (figs. 1(c), 2(c), and 3(c)) have been nondimensionalized by the quantity ω_{30} and not by the total rotational velocity magnitude ω_0 . A false impression of the effect of coning angle on the cable tension may be given if these figures are not interpreted properly. If it is desired to obtain the change in cable tension because of a change in the coning angle for a fixed value of the magnitude of the angular rotation vector, a nondimensionalization based on the quantity ω_0 should be used. A simple conversion for altering the nondimensional form is

$$\frac{2a\sqrt{1 + \frac{I}{K}}}{I_3\omega_0^2} T = C\tilde{T}$$

where

$$C = \frac{1}{1 + (I \tan \Gamma_0)^2} \quad (19)$$

If this conversion factor is used for the case presented in figure 3(c) and for $\tau = 0.6$, the value of nondimensional tension based on ω_0^2 rather than ω_{30}^2 for $\Gamma_0 = 50^\circ$ is 0.7 as

compared with 2.35 for \tilde{T} . Therefore, when compared with the $\Gamma_0 = 0$ case, it is observed that for a given value of the total rotational magnitude ω_0 , the cable tension decreases with increasing initial coning angle.

In figures 4, 5, and 6, four parameters of basic interest for the design of a despin system are presented as a function of the ratio K/I for various values of the initial coning angle. These curves represent the three basic geometries $I = 0.1, 0.9$ and 1.3 . Values of $\tilde{\omega}_{12}$, τ , and $\tilde{\beta}$ at the instant when $\tilde{\omega}_3$ is zero are presented along with the maximum value of the nondimensional cable tension.

In figures 5 and 6 an absence of data for $\Gamma_0 = 50^\circ$ may be noticed. This lack is due to the occurrence of the rewinding phenomena ($\beta = \beta_{\max}$) mentioned previously and shown in figure 2. Also, in figures 5 and 6, some of the curves are dotted and some dashed for reading clarity in the rather congested area at low values of K/I .

The quantity $\tilde{\omega}_{12}$ at $\omega_3 = 0$ represents the residual tumbling rate of the system and its variation with Γ_0 and K/I are given in figures 4(a), 5(a), and 6(a) for the three values of I considered. For $I = 0.1$, this final cross-axis spin rate is independent of the inertia ratio parameter for all values of the initial coning angle up to 50° ; however, for $I = 0.9$ and 1.3 , the design problem is a little more sensitive, especially at the lower values of K .

The nondimensional despin time is shown in figures 4(b), 5(b), and 6(b). This parameter can be important, for instance, when the despin of spinning atmospheric entry probes is being considered. It is seen again that for $I = 0.1$ the two-dimensional despin time ($\Gamma_0 = 0^\circ$) is a very good estimation of the three-dimensional despin time except when K/I is chosen very small and Γ_0 is large. For the larger values of I , the despin time would be grossly in error if the two-dimensional results were used where there was a significant amount of coning.

The maximum nondimensional cable tension shown in figures 4(c), 5(c), and 6(c) is also very near the two-dimensional value for $I = 0.1$ except when K/I is very small, whereas at the larger values of I both initial coning angle and changes in K produce large variations in this parameter.

The parameter $\tilde{\beta}$ at $\omega_3 = 0$ represents the nondimensional cable length required for despin and is plotted in figures 4(d), 5(d), and 6(d). The variations of this parameter for changes in Γ_0 and K are again small for $I = 0.1$ but grow larger for the larger values of I .

In general, figures 4, 5, and 6 show that for a slender body ($I = 0.1$), the two-dimensional theory is probably sufficient for most engineering purposes unless very small despin weights or very small values of a are desired, whereas for more disk-like bodies

($I = 0.9$ and 1.3), a more thorough analysis should be made, especially when large coning angles or small values of K are to be encountered.

CONCLUDING REMARKS

Integration of the equations which describe the three-dimensional motion of a spinning rigid body during the yo-yo despin process must be done numerically because no general analytical solutions to these equations have been derived. This paper presents the equations and their derivation and points out that special precaution must be taken at the beginning of the numerical integration procedure because of a singularity in the coefficient matrix of the differential equations at the initial instant of motion. A convenient method of nondimensionalization is also presented which allows the reduction of the parameters necessary for integration to be reduced to four: inertia ratio of body I , inertia factor for despin weights K , initial angular velocity ratio ω_{20}/ω_{10} , and initial coning angle Γ_0 . An analysis of some particular cases shows that despin time, cable tension, and cable length may be computed with good accuracy by the two-dimensional approximations for some range of Γ_0 and K/I for all the values of the inertia ratio I studied. For $I = 0.1$, it is found that the two-dimensional approximations hold very well for all Γ_0 if the ratio K/I is above 0.02. For $I = 0.9$ and 1.3 , it is found that the range of applicability of the two-dimensional results should be restricted to values of Γ_0 of about 10° to 20° depending upon the accuracy which is required.

In every case studied herein, the cross-axis spin rate after despin is found to be less than or equal to its initial value, and therefore, it appears that the yo-yo device also has a damping effect on this component of the angular velocity vector.

For this study of the tangential despin, the value of the angle α did not increase beyond the value of the initial coning angle for the three time histories presented and did not reach a value of 90° for any of the cases integrated.

An important point should also be made here concerning the length of cable required to despin the body. It can be observed that the nondimensional cable length $\tilde{\beta}$ required to despin is very sensitive to both the coning angle and the ratio K/I . A slight misjudgment of this value could lead to serious difficulties if some initial coning exists. For instance, if the cable length is designed from two-dimensional considerations, it may be too long and may not unwind and release properly.

Langley Research Center,

National Aeronautics and Space Administration,

Langley Station, Hampton, Va., September 7, 1966,

124-07-02-35-23.

APPENDIX A

DERIVATION OF THE EQUATIONS OF MOTION OF A DESPIN WEIGHT

In the paper, it was pointed out that the equations of motion of a despin weight can be written as

$$-\hat{T} = m \frac{d^2 \hat{r}}{dt^2}$$

where

$$\hat{r} = r_1 \hat{i} + r_2 \hat{j} + r_3 \hat{k} \quad (A1)$$

and r_1 , r_2 , and r_3 are given in equations (2) and \hat{T} is found in equation (3). In this appendix the nondimensional forms of these parameters are used and, therefore, equation (12) of the main text is derived here rather than equation (9).

The nondimensional radius vector $\hat{\tilde{r}}$ is formed as

$$\hat{\tilde{r}} = \frac{\hat{r}}{a} \quad (A2)$$

When derivatives are taken in terms of the nondimensional time τ in place of t , the following substitutions may be made

$$(\cdot) = (\cdot)' \frac{d\tau}{dt}$$

or using the definitions of equations (10)

$$(\cdot) = (\cdot)' \frac{\omega_{30}}{\sqrt{1 + \frac{I}{K}}} \quad (A3)$$

also,

$$(\ddot{\cdot}) = (\cdot)'' \frac{\omega_{30}^2}{1 + \frac{I}{K}} \quad (A4)$$

Equation (7) may be rewritten as

$$-\frac{I_3 \omega_{30}^2}{2a \sqrt{1 + \frac{I}{K}}} \hat{\tilde{T}} = ma \frac{d^2 \hat{\tilde{r}}}{d\tau^2} \frac{\omega_{30}^2}{1 + \frac{I}{K}}$$

APPENDIX A

or

$$-\hat{T} = \frac{K}{I\sqrt{1 + \frac{I}{K}}} \frac{d^2 \hat{r}}{d\tau^2} \quad (A5)$$

It is found convenient for computations to introduce another nondimensional form for the angular rotation vector $\hat{\omega}$

$$\hat{\omega}^* = \sqrt{1 + \frac{I}{K}} \hat{\omega} \quad (A6)$$

The derivatives of the vector \hat{r} can be formed in the following manner:

$$\hat{V} = \frac{d\hat{r}}{d\tau} = \hat{r}' + \hat{\omega}^* \times \hat{r}$$

or

$$\left. \begin{aligned} \tilde{V}_1 &= \tilde{r}'_1 + \tilde{\omega}_2^* \tilde{r}_3 - \tilde{\omega}_3^* \tilde{r}_2 \\ \tilde{V}_2 &= \tilde{r}'_2 + \tilde{\omega}_3^* \tilde{r}_1 - \tilde{\omega}_1^* \tilde{r}_3 \\ \tilde{V}_3 &= \tilde{r}'_3 + \tilde{\omega}_1^* \tilde{r}_2 - \tilde{\omega}_2^* \tilde{r}_1 \end{aligned} \right\} \quad (A7)$$

The relative derivatives of the components of \hat{r} are found from

$$\tilde{r}'_i = \tilde{r}_{i\beta} \beta' + \tilde{r}_{i\alpha} \alpha' \quad (i = 1, 2, \text{ and } 3) \quad (A8)$$

and from equations (2) of the main text

$$\left. \begin{aligned} \tilde{r}_{1\beta} &\equiv \frac{\partial \tilde{r}_1}{\partial \beta} = \sin \beta \cos \alpha - \tilde{r}_2 \\ \tilde{r}_{2\beta} &\equiv \frac{\partial \tilde{r}_2}{\partial \beta} = \tilde{r}_1 - \cos \beta \cos \alpha \\ \tilde{r}_{3\beta} &\equiv \frac{\partial \tilde{r}_3}{\partial \beta} = -\sin \alpha \\ \tilde{r}_{1\alpha} &\equiv \frac{\partial \tilde{r}_1}{\partial \alpha} = \tilde{r}_3 \sin \beta \\ \tilde{r}_{2\alpha} &\equiv \frac{\partial \tilde{r}_2}{\partial \alpha} = -\tilde{r}_3 \cos \beta \\ \tilde{r}_{3\alpha} &\equiv -\beta \cos \alpha \end{aligned} \right\} \quad (A9)$$

APPENDIX A

The "absolute" acceleration is then

$$\hat{\ddot{A}} = \frac{d^2 \hat{\tilde{r}}}{d\tau^2} = \hat{\dot{\tilde{r}}} + \hat{\tilde{\omega}}^* \times \hat{\tilde{r}} + \hat{\tilde{\omega}}^* \times \hat{\tilde{r}} + \hat{\tilde{\omega}}^* \times \hat{\tilde{V}} \quad (\text{A10})$$

The "relative" acceleration of $\hat{\tilde{r}}$ is needed and is

$$\hat{\tilde{r}}' = \tilde{r}_i'' = \tilde{r}_{i\beta}'' + \tilde{r}_{i\alpha}'' + \tilde{r}_{i\beta}'\beta' + \tilde{r}_{i\alpha}'\alpha' \quad (i = 1, 2, \text{ and } 3) \quad (\text{A11})$$

where

$$\left. \begin{aligned} \tilde{r}_{1\beta}' &= (\cos \beta \cos \alpha - \tilde{r}_{2\beta})\beta' - (\sin \beta \sin \alpha + \tilde{r}_{2\alpha})\alpha' \\ \tilde{r}_{2\beta}' &= (\tilde{r}_{1\beta} + \sin \beta \cos \alpha)\beta' + (\tilde{r}_{1\alpha} + \cos \beta \sin \alpha)\alpha' \\ \tilde{r}_{3\beta}' &= -(\cos \alpha)\alpha' \\ \tilde{r}_{1\alpha}' &= (\tilde{r}_{3\beta} \sin \beta + \tilde{r}_3 \cos \beta)\beta' + (\tilde{r}_{3\alpha} \sin \beta)\alpha' \\ \tilde{r}_{2\alpha}' &= (\tilde{r}_3 \sin \beta - \tilde{r}_{3\beta} \cos \beta)\beta' - (\tilde{r}_{3\alpha} \cos \beta)\alpha' \\ \tilde{r}_{3\alpha}' &= -(\cos \alpha)\beta' + (\beta \sin \alpha)\alpha' \end{aligned} \right\} \quad (\text{A12})$$

In equation (A10) the Coriolis and centripetal accelerations may be written together as C_i where

$$\left. \begin{aligned} C_1 &= \tilde{\omega}_2^* \tilde{r}_3' - \tilde{\omega}_3^* \tilde{r}_2' + \tilde{\omega}_2^* \tilde{V}_3 - \tilde{\omega}_3^* \tilde{V}_2 \\ C_2 &= \tilde{\omega}_3^* \tilde{r}_1' - \tilde{\omega}_1^* \tilde{r}_3' + \tilde{\omega}_3^* \tilde{V}_1 - \tilde{\omega}_1^* \tilde{V}_3 \\ C_3 &= \tilde{\omega}_1^* \tilde{r}_2' - \tilde{\omega}_2^* \tilde{r}_1' + \tilde{\omega}_1^* \tilde{V}_2 - \tilde{\omega}_2^* \tilde{V}_1 \end{aligned} \right\} \quad (\text{A13})$$

and the Euler terms

$$\left. \begin{aligned} E_1 &= \tilde{\omega}_2^* \tilde{r}_3 - \tilde{\omega}_3^* \tilde{r}_2 \\ E_2 &= \tilde{\omega}_3^* \tilde{r}_1 - \tilde{\omega}_1^* \tilde{r}_3 \\ E_3 &= \tilde{\omega}_1^* \tilde{r}_2 - \tilde{\omega}_2^* \tilde{r}_1 \end{aligned} \right\} \quad (\text{A14})$$

If the Euler equations are used as given in equations (11) along with the definition in equation (A6), the derivatives $\tilde{\omega}_i^*$ may be replaced in equation (A14) by the variables $\tilde{\omega}_i$, $\tilde{\beta}$, $\tilde{\alpha}$, and \tilde{T} . Also if the main text of this paper is referred to for the components of $\hat{\tilde{T}}$,

APPENDIX A

the derivatives and other expressions derived in this appendix may be manipulated to obtain an expression in the form of equation (12) or

$$\sum_{j=1}^3 \tilde{a}_{ij} \tilde{X}_j = \tilde{b}_i \quad (i = 1, 2, \text{ and } 3) \quad (\text{A15})$$

where \tilde{X}_i corresponds to $\tilde{\beta}'$, $\tilde{\alpha}'$, and \tilde{T} and

$$\tilde{a}_{11} = \tilde{r}_{1\beta}$$

$$\tilde{a}_{12} = \tilde{r}_{1\alpha}$$

$$\tilde{a}_{13} = \frac{I}{K} \sin \beta \cos \alpha + I \tilde{r}_3 \sin \alpha \cos \beta + \tilde{r}_2 \cos \alpha$$

$$\tilde{a}_{21} = \tilde{r}_{2\beta}$$

$$\tilde{a}_{22} = \tilde{r}_{2\alpha}$$

$$\tilde{a}_{23} = -\frac{I}{K} \cos \beta \cos \alpha - \tilde{r}_1 \cos \alpha + I \tilde{r}_3 \sin \alpha \sin \beta$$

$$\tilde{a}_{31} = \tilde{r}_{3\beta}$$

$$\tilde{a}_{32} = \tilde{r}_{3\alpha}$$

$$\tilde{a}_{33} = -\frac{I}{K} \sin \alpha - I \tilde{r}_2 \sin \alpha \sin \beta - I \tilde{r}_1 \sin \alpha \cos \beta$$

$$\tilde{b}_1 = \left[-C_1 - \tilde{r}'_{1\beta} \beta' - \tilde{r}'_{1\alpha} \alpha' + \tilde{r}_3 (1 - I) \tilde{\omega}_1^* \tilde{\omega}_3^* \right] \frac{1}{\sqrt{1 + \frac{I}{K}}}$$

$$\tilde{b}_2 = \left[-C_2 - \tilde{r}'_{2\beta} \beta' - \tilde{r}'_{2\alpha} \alpha' + \tilde{r}_3 (1 - I) \tilde{\omega}_2^* \tilde{\omega}_3^* \right] \frac{1}{\sqrt{1 + \frac{I}{K}}}$$

$$\tilde{b}_3 = \left[-C_3 - \tilde{r}'_{3\beta} \beta' - \tilde{r}'_{3\alpha} \alpha' - \tilde{r}_2 (1 - I) \tilde{\omega}_2^* \tilde{\omega}_3^* - \tilde{r}_1 (1 - I) \tilde{\omega}_1^* \tilde{\omega}_3^* \right] \frac{1}{\sqrt{1 + \frac{I}{K}}}$$

where α and β may be written in terms of $\tilde{\alpha}$ and $\tilde{\beta}$ by use of equations (10) and $\tilde{\omega}^*$ may be rewritten by equation (A6). These expressions give the information required to integrate the governing equations (12).

APPENDIX B

INITIAL CONDITIONS

The conditions which must be satisfied at the initial instant are: (1) the velocity of the despin weights relative to the body is initially zero and (2) the unwind angle β is also zero. The angle α at the initial instant is not prespecified by the choice of coordinates. However, when the conditions $\dot{\mathbf{r}}_0 = 0$ and $\beta_0 = 0$ are applied, it is found the $\alpha_0 = 0$ is a necessary initial condition. Furthermore, when these conditions are applied to the coefficient matrix in equations (12), all the elements \tilde{a}_{ij} are found to be zero except \tilde{a}_{23} which is the coefficient of the initial nondimensional cable tension \tilde{T} in the second equation. Equations (12) then provide the following expressions which must be valid at the initial instant:

$$\left. \begin{aligned} \tilde{\beta}'_0 &= \sqrt{(\tilde{\omega}_{20})^2 + 1} \\ \tilde{T}_0 &= \frac{\tilde{\omega}_{10}\tilde{\omega}_{20}}{\sqrt{1 + \frac{I}{K}}} \\ \tilde{\alpha}'_0 &= \frac{2 - I}{2\tilde{\beta}'_0} \tilde{\omega}_{10} \end{aligned} \right\} \quad (B1)$$

If it is noted that

$$\tilde{\omega}_{30} = 1$$

it can be observed that if I , K , $\tilde{\omega}_{10}$, and $\tilde{\omega}_{20}$ are known, the initial values of all the other quantities $\tilde{\alpha}_0$, $\tilde{\beta}_0$, $\tilde{\alpha}'_0$, $\tilde{\beta}'_0$, and \tilde{T}_0 are specified. The fact that only four quantities are necessary to specify the motion of this system leads to reductions in the amount of effort required to present the data.

Equations (15) could now be integrated if it were not for the fact that the matrix of elements \tilde{a}_{ij} is singular at the initial instant and therefore \tilde{T} , y'_6 , and y'_7 cannot be computed initially. It is, therefore, necessary to find other expressions which will be valid at the initial instant. This procedure has already been done for T_0 as was shown in equations (B1). The initial values of y'_6 and y'_7 , which correspond to $\tilde{\beta}'_0$ and $\tilde{\alpha}'_0$, are found by differentiating equations (12) with respect to the nondimensional time τ and applying the initial conditions which are given. When this is done, two relations valid at the initial instant are found

$$\left. \begin{aligned} \tilde{a}'_{11}\tilde{\beta}'_0 + \tilde{a}'_{12}\tilde{\alpha}'_0 &= \tilde{b}'_1 - \tilde{a}'_{13}\tilde{T}_0 \\ \tilde{a}'_{31}\tilde{\beta}'_0 + \tilde{a}'_{32}\tilde{\alpha}'_0 &= \tilde{b}'_3 - \tilde{a}'_{33}\tilde{T}_0 \end{aligned} \right\} \quad (B2)$$

APPENDIX B

After taking the appropriate derivatives and manipulating, the desired initial conditions are found to be

$$\left. \begin{aligned} \tilde{\beta}'_0 &= \frac{2}{\tilde{\beta}_0} (\tilde{\omega}_{20} \tilde{\omega}'_{20} + \tilde{\omega}'_{30}) + \frac{4\sqrt{1+\frac{I}{K}}}{3} \tilde{\alpha}'_0 \tilde{\omega}_{20} - \frac{I}{3K} \tilde{T}_0 \\ \tilde{\alpha}'_0 &= -\frac{\tilde{\alpha}_0}{\tilde{\beta}_0} \tilde{\beta}'_0 + \frac{2-I}{3\tilde{\beta}_0} (\tilde{\omega}'_{10} + \tilde{\omega}_{10} \tilde{\omega}'_{30}) - \frac{2\sqrt{1+\frac{I}{K}}}{3} \tilde{\beta}'_0 \tilde{\omega}_{20} - \frac{I(1+K)}{3K} \frac{\tilde{\alpha}_0}{\tilde{\beta}_0} \tilde{T}_0 \end{aligned} \right\} \quad (B3)$$

which are the initial values of the quantities y'_6 and y'_7 in equations (15), and the values of $\tilde{\omega}'_{10}$, $\tilde{\omega}'_{20}$, and $\tilde{\omega}'_{30}$ may be found from equations (11) at the initial instant. These sets of initial conditions are used to start the integration and once started, equations (15) are integrated by a standard fourth-order Runge-Kutta numerical integration technique.

In place of presenting initial conditions in terms of $\tilde{\omega}_{10}$ and $\tilde{\omega}_{20}$, it was decided that the initial coning angle Γ_0 and the ratio $\tilde{\omega}_{20}/\tilde{\omega}_{10}$ would be more significant and, therefore, these quantities are the parameters which represent the initial conditions in the data presented. If Γ_0 and ω_{20}/ω_{10} are given initial conditions, the quantities $\tilde{\omega}_{10}$ and $\tilde{\omega}_{20}$ must be determined from them so that equations (15) may be integrated. By noting that

$$\frac{\tilde{\omega}_{20}}{\tilde{\omega}_{10}} = \frac{\omega_{20}}{\omega_{10}}$$

and by equations (16) and (17), the component of the nondimensional angular velocity vector along the x_1 body axis at the initial instant is

$$\tilde{\omega}_{10} = \epsilon \frac{I \tan \Gamma_0}{\sqrt{1 + \left(\frac{\omega_{20}}{\omega_{10}}\right)^2}} \quad (B4)$$

and the x_2 component

$$\tilde{\omega}_{20} = \left(\frac{\omega_{20}}{\omega_{10}}\right) \tilde{\omega}_{10} \quad (B5)$$

The ϵ in equation (B4) is chosen as positive or negative unity so that the $\tilde{\omega}_{120}$ component of the angular rotation vector is put into the appropriate quadrant in the x_1, x_2

APPENDIX B

plane. For this study it is assumed without loss of generality that the x_1 , x_2 , and x_3 coordinate system is chosen so that at the initial instant, the parameter $\tilde{\omega}_{20}$ is positive. In this case ϵ is determined by

$$\epsilon = \text{sgn}\left(\frac{\omega_{20}}{\omega_{10}}\right) \quad (\text{B6})$$

REFERENCES

1. Counter, Duane N.: Spin Reduction for Ion Probe Satellite S-30 (19D). MNN-M-G&C-5-60, Marshall Space Flight Center, Sept. 12, 1960.
2. Fedor, J. V.: Theory and Design Curves for a Yo-Yo De-Spin Mechanism for Satellites. NASA TN D-708, 1961.
3. Curfman, Howard; McKee, Thomas; and Youngblood, James: Derivation of Angular-Velocity Ratio for a Particular Despin System. J. Aerospace Sci. (Readers Forum), vol. 28, no. 10, Oct. 1961, pp. 822-823.
4. Eide, Donald G.; and Vaughan, Chester A.: Equations of Motion and Design Criteria for the Despin of a Vehicle by the Radial Release of Weights and Cables of Finite Mass. NASA TN D-1012, 1962.
5. Cornille, Henry J., Jr.: A Method of Accurately Reducing the Spin Rate of a Rotating Spacecraft. NASA TN D-1420, 1962.
6. Fedor, Joseph V.: Analytical Theory of the Stretch Yo-Yo for Despin of Satellites. NASA TN D-1676, 1963.
7. Mentzer, William R.: Analysis of the Dynamic Tests of the Stretch Yo-Yo De-Spin System. NASA TN D-1902, 1963.
8. Williams, H. E.: On the Motion of a Slender Rigid Body Caused by a Small Torque. Tech. Rept. No. 32-62, Jet Propulsion Lab., California Inst. Technol., March 10, 1961.
9. Goldstein, Herbert: Classical Mechanics. Addison-Wesley Pub. Co., Inc. (Reading, Mass.), c.1959.
10. Synge, J. L.; and Griffith, B. A.: Principles of Mechanics. McGraw-Hill Book Co., Inc., c.1942.
11. Collins, Robert L.: On the Motion of a Symmetric Rigid Body With a "Yo-Yo" Despin Device Attached. PhD. Thesis, Virginia Polytechnic Institute, June 1966.

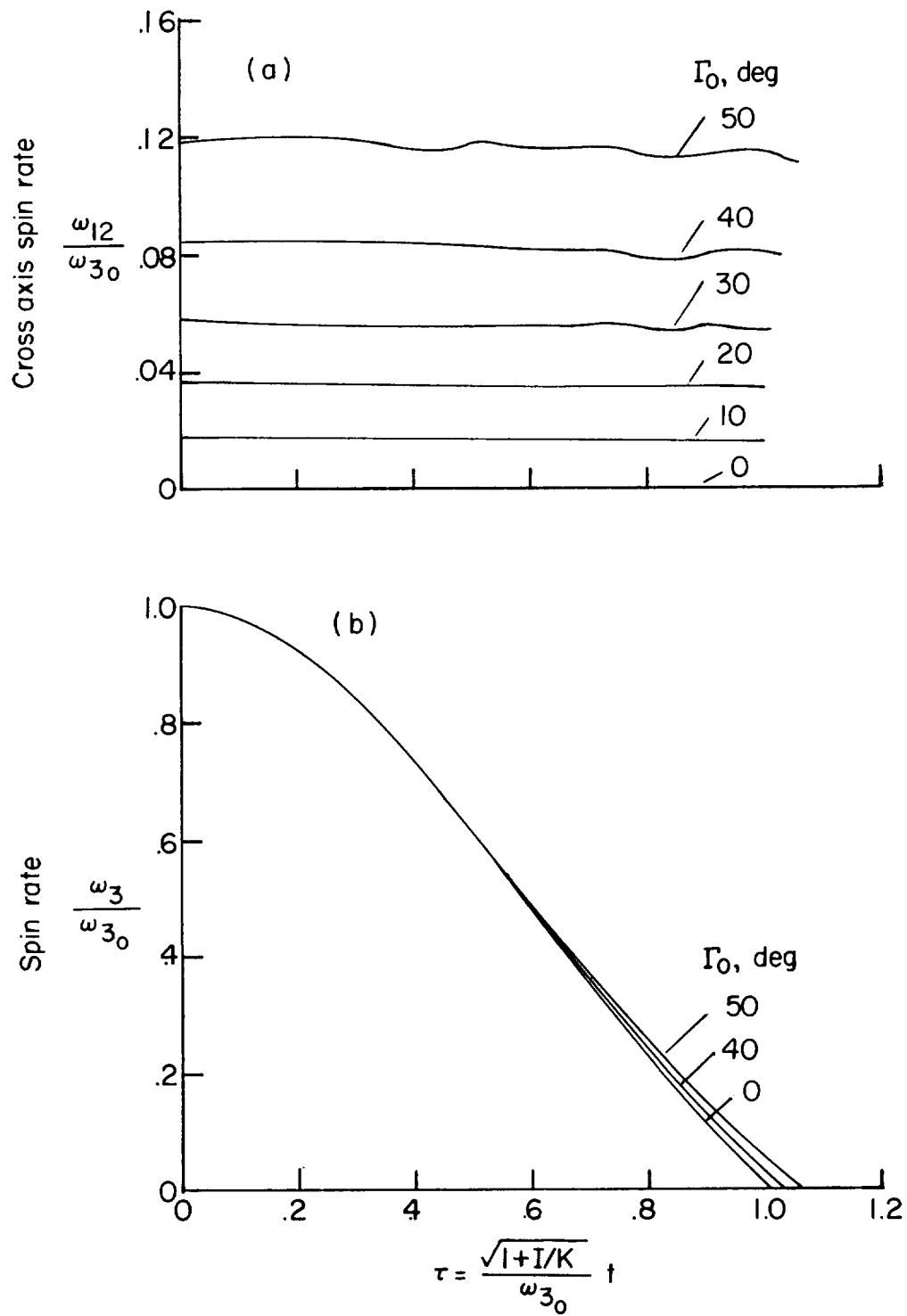


Figure 1.- Parameters of motion plotted against time in nondimensional form for various values of the initial coning angle and for $I = 0.1$, $K = 0.001$.

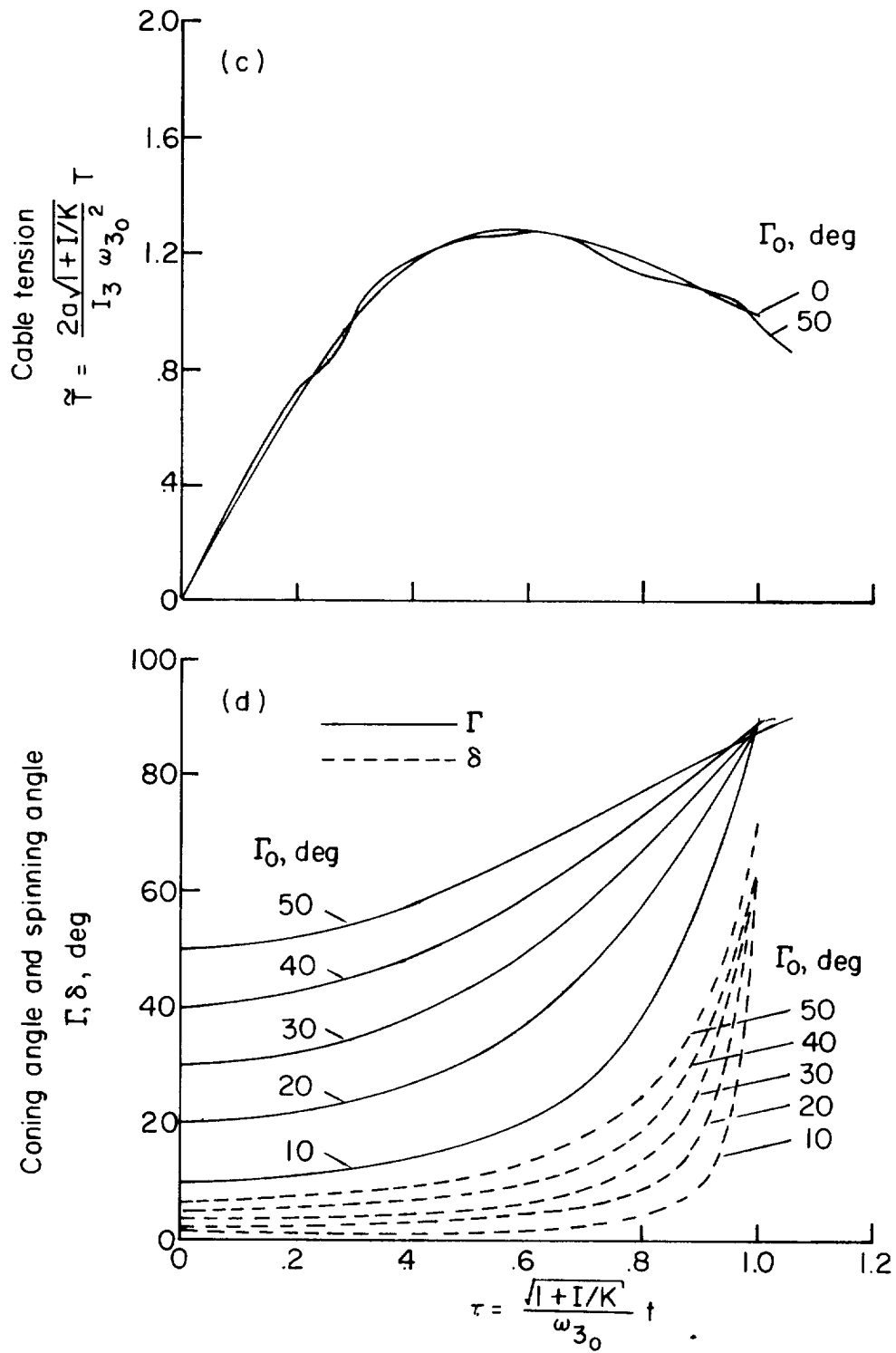


Figure 1.- Continued.

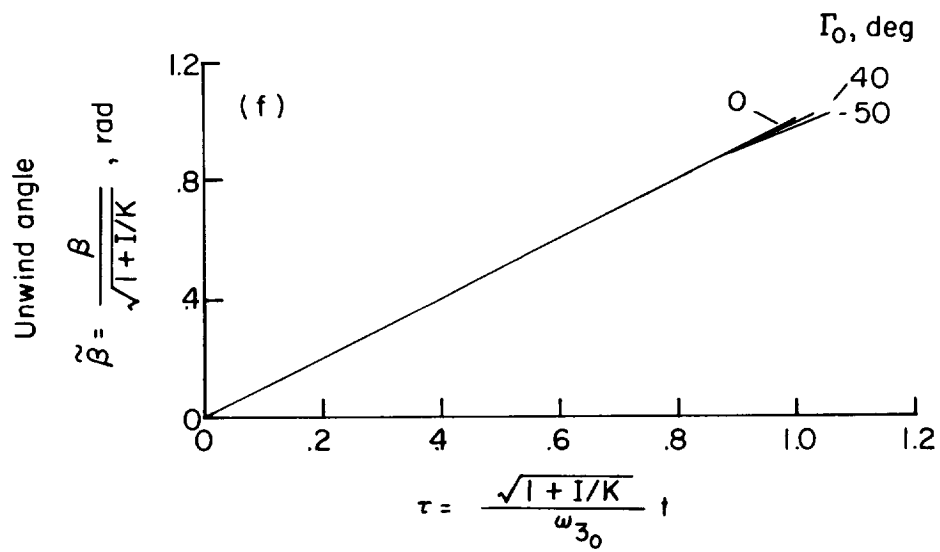
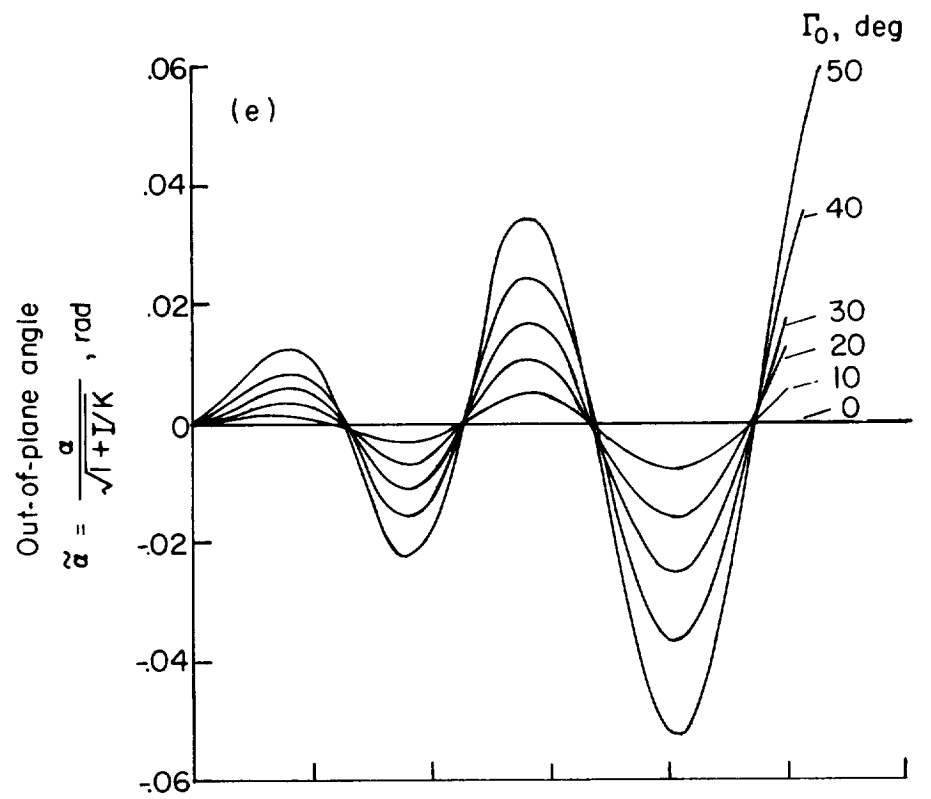


Figure 1.- Concluded.

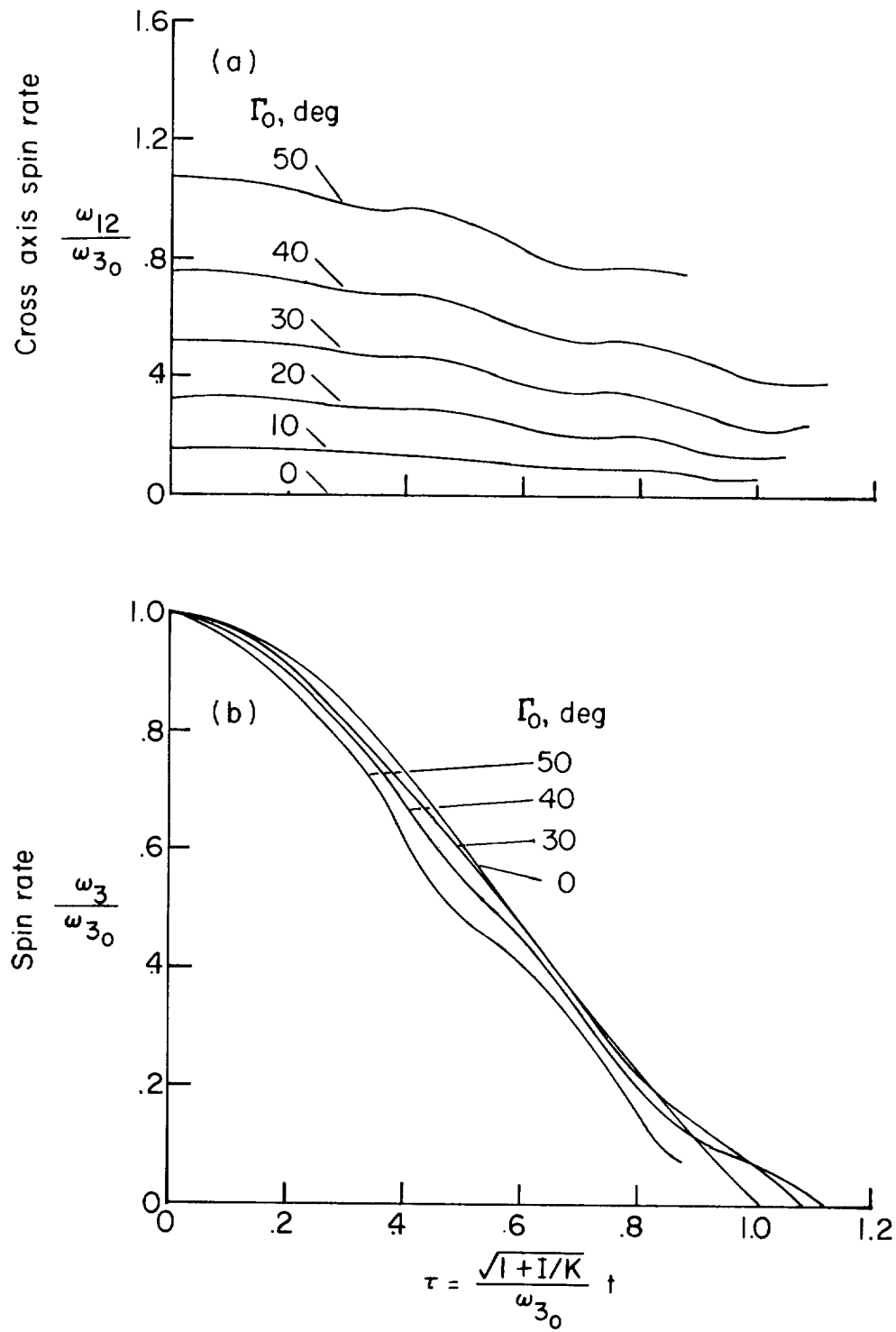


Figure 2.- Parameters of motion plotted against time in nondimensional form for various values of initial coning angle and for $I = 0.9$, $K = 0.01$.

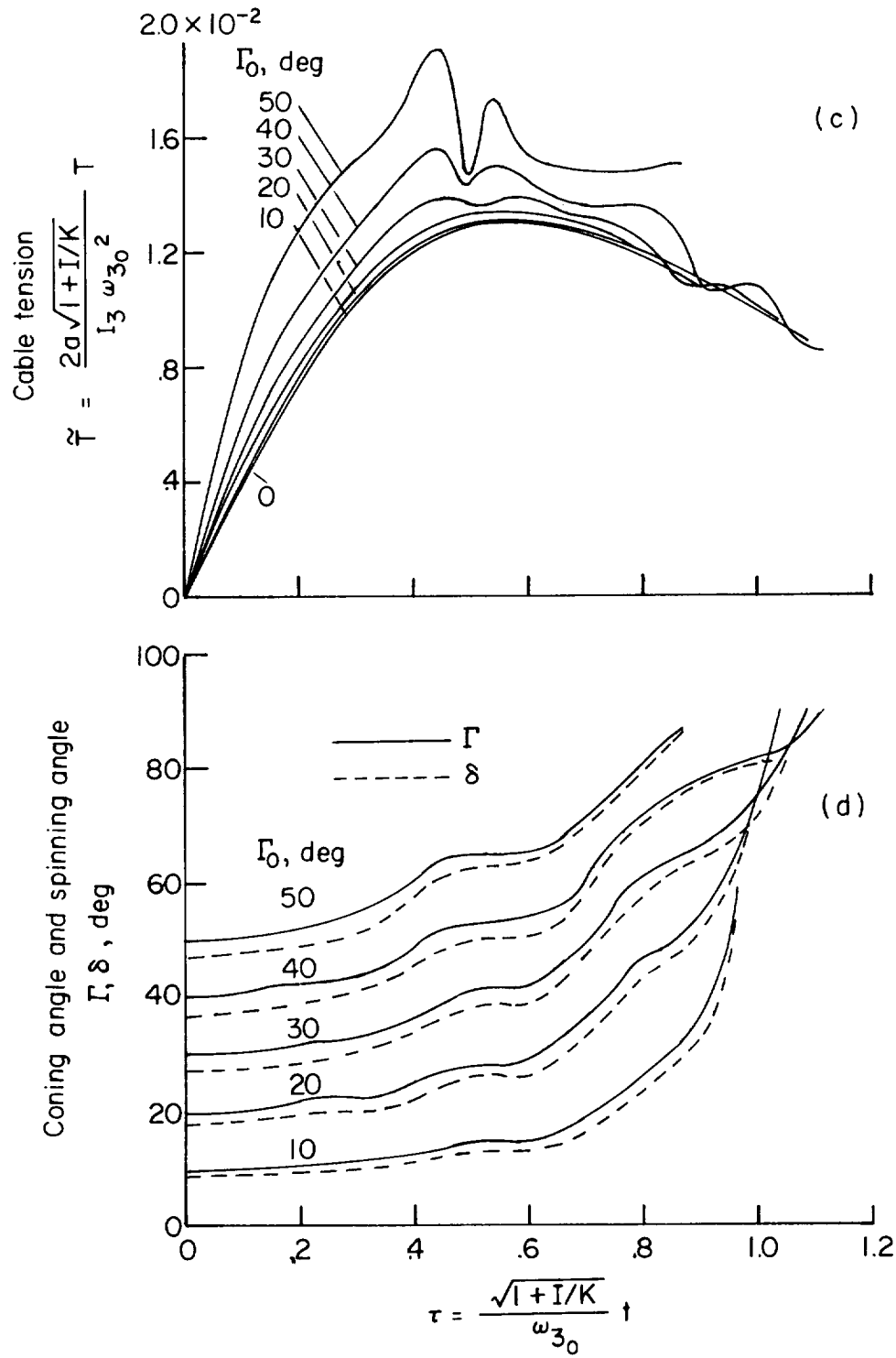


Figure 2.- Continued.

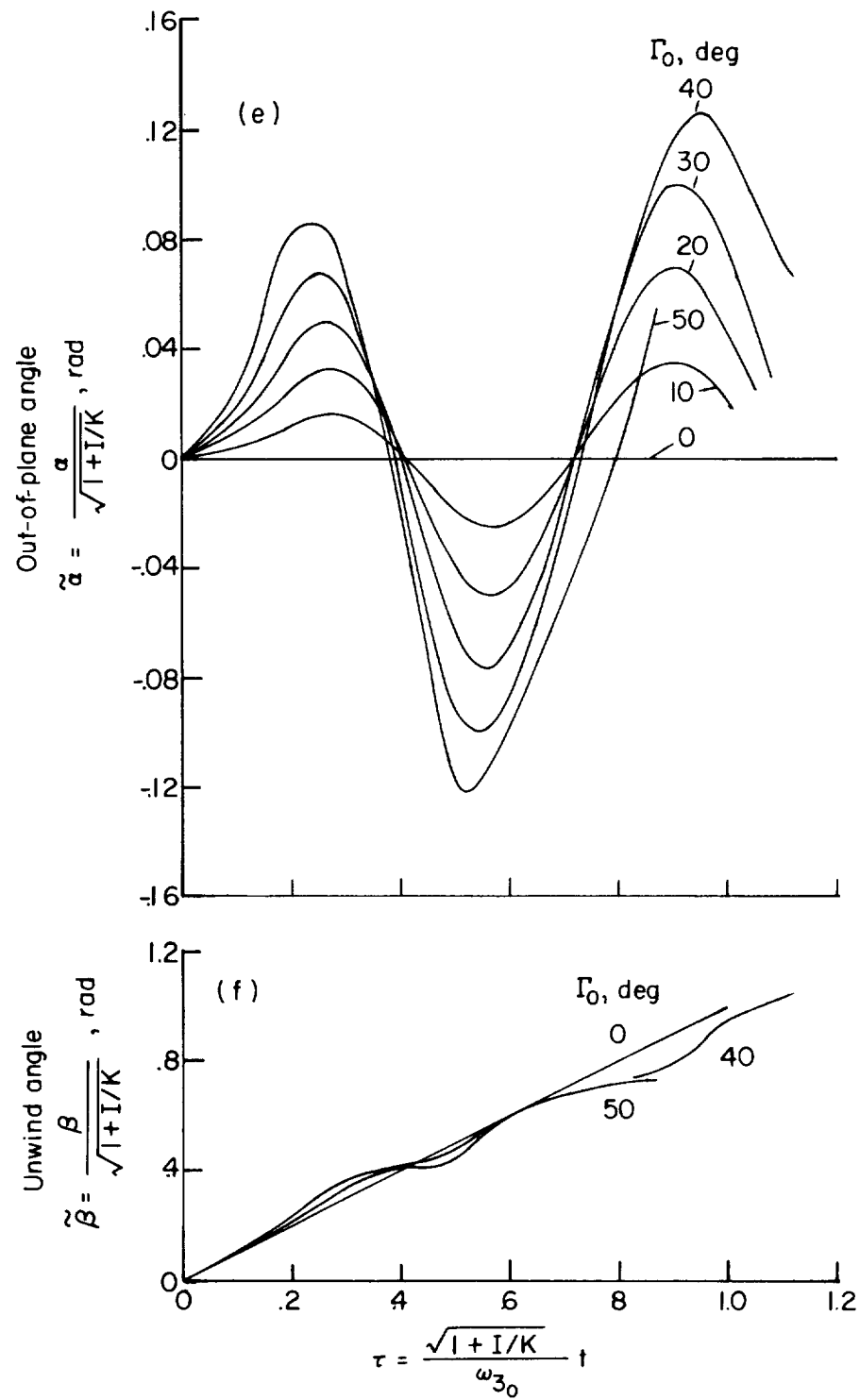


Figure 2.- Concluded.

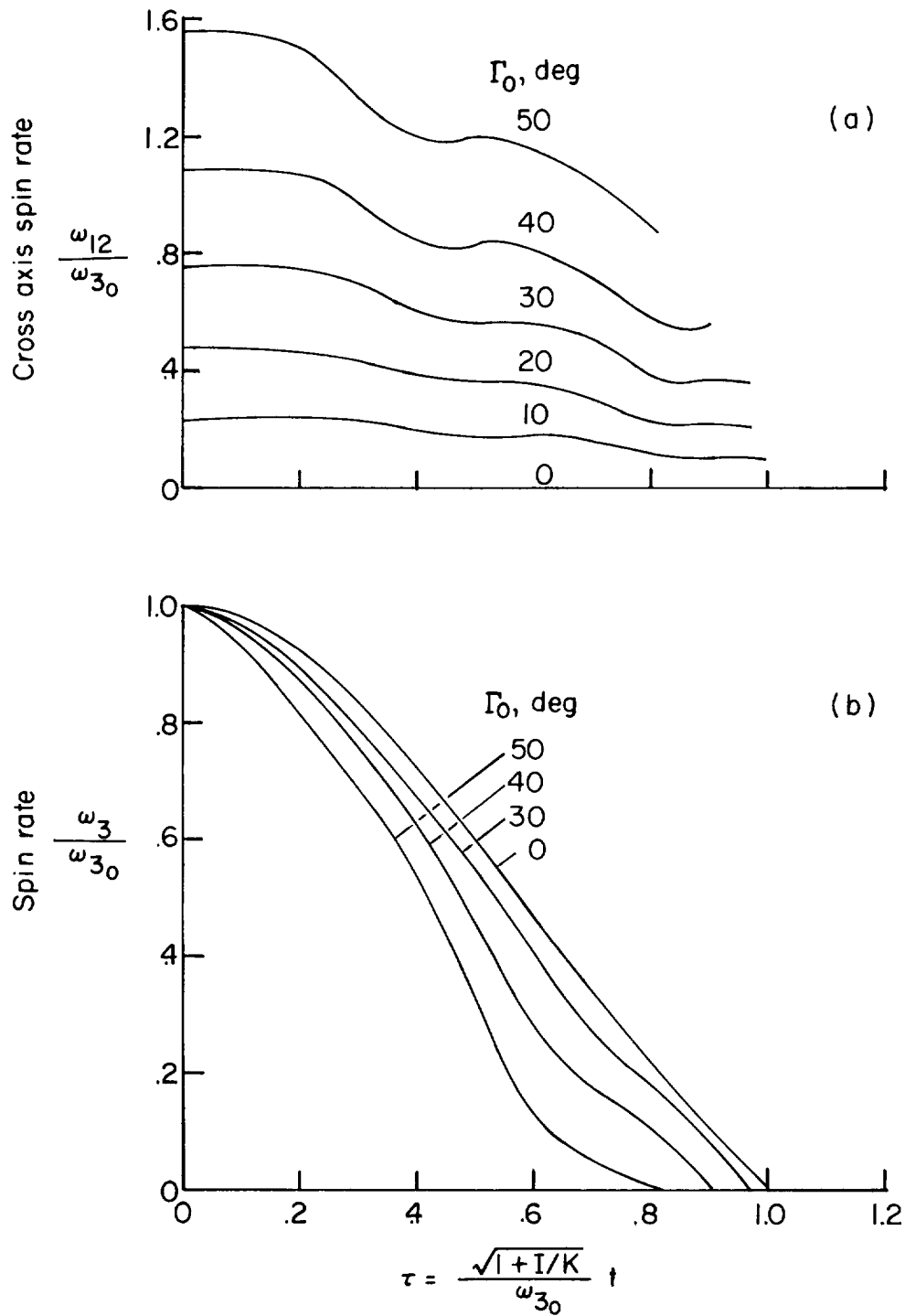


Figure 3.- Parameters of motion plotted against time in nondimensional form for various values of initial coning angle and for $I = 1.3$, $K = 0.015$.

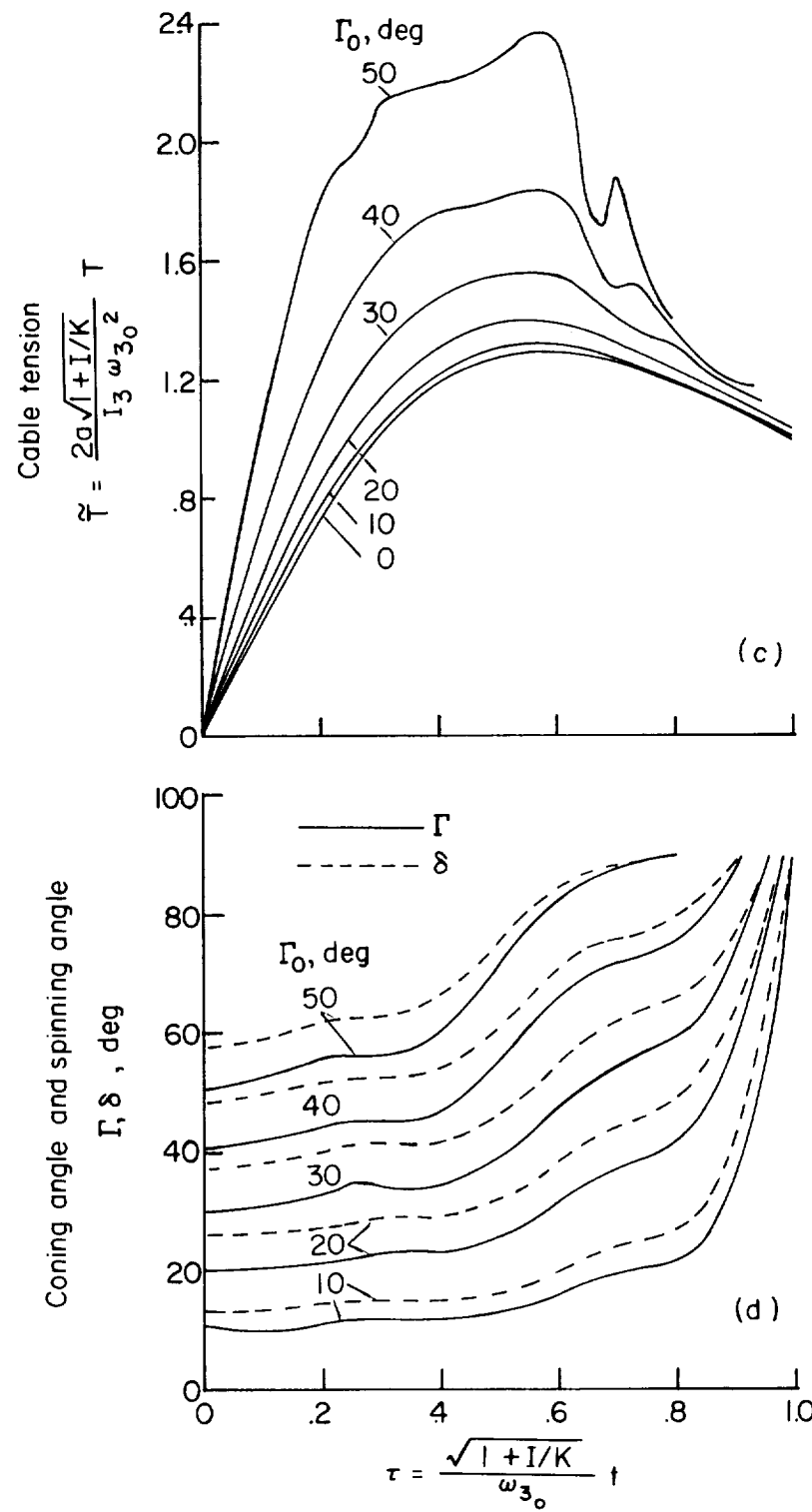


Figure 3.- Continued.

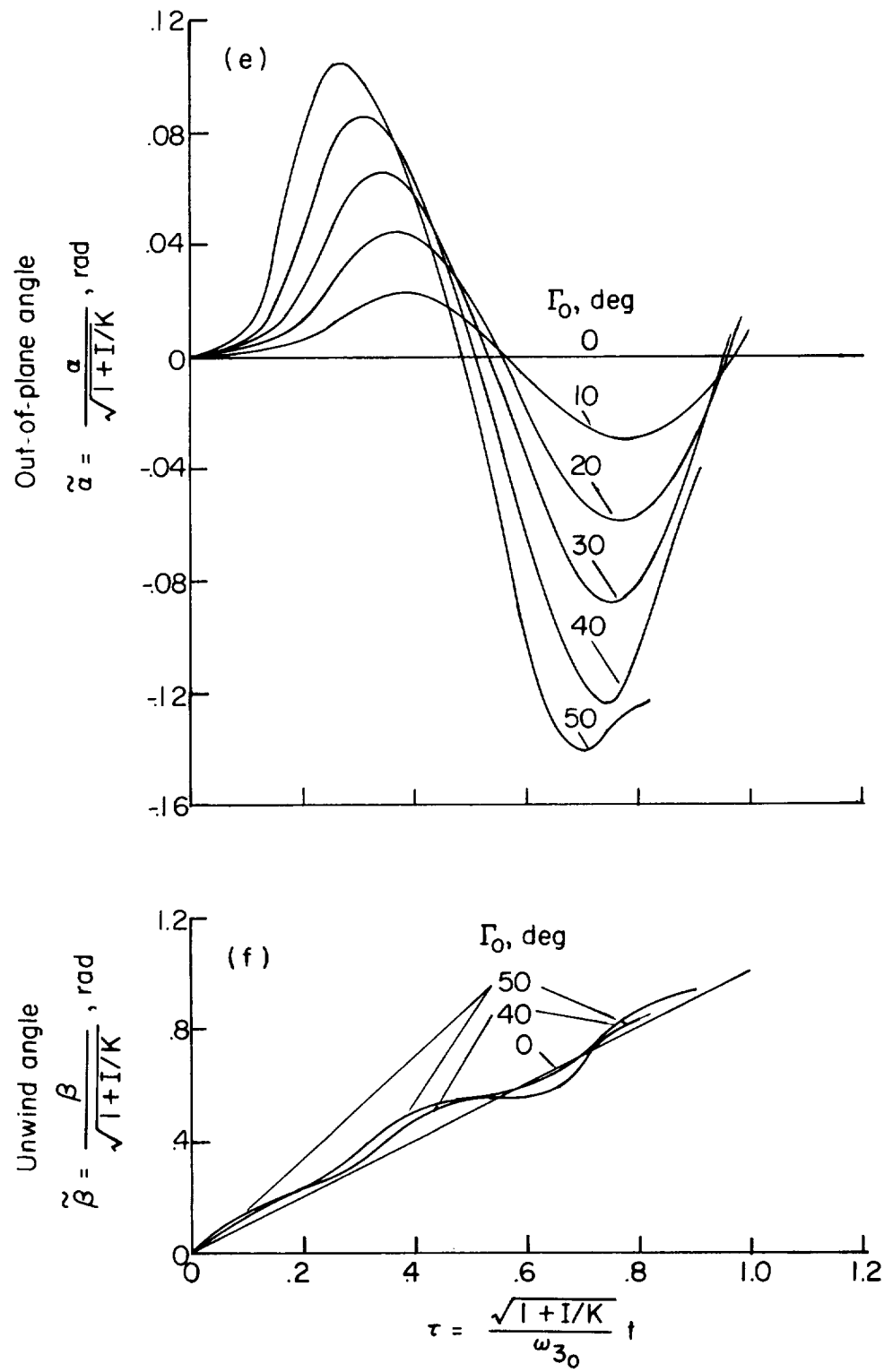


Figure 3.- Concluded.

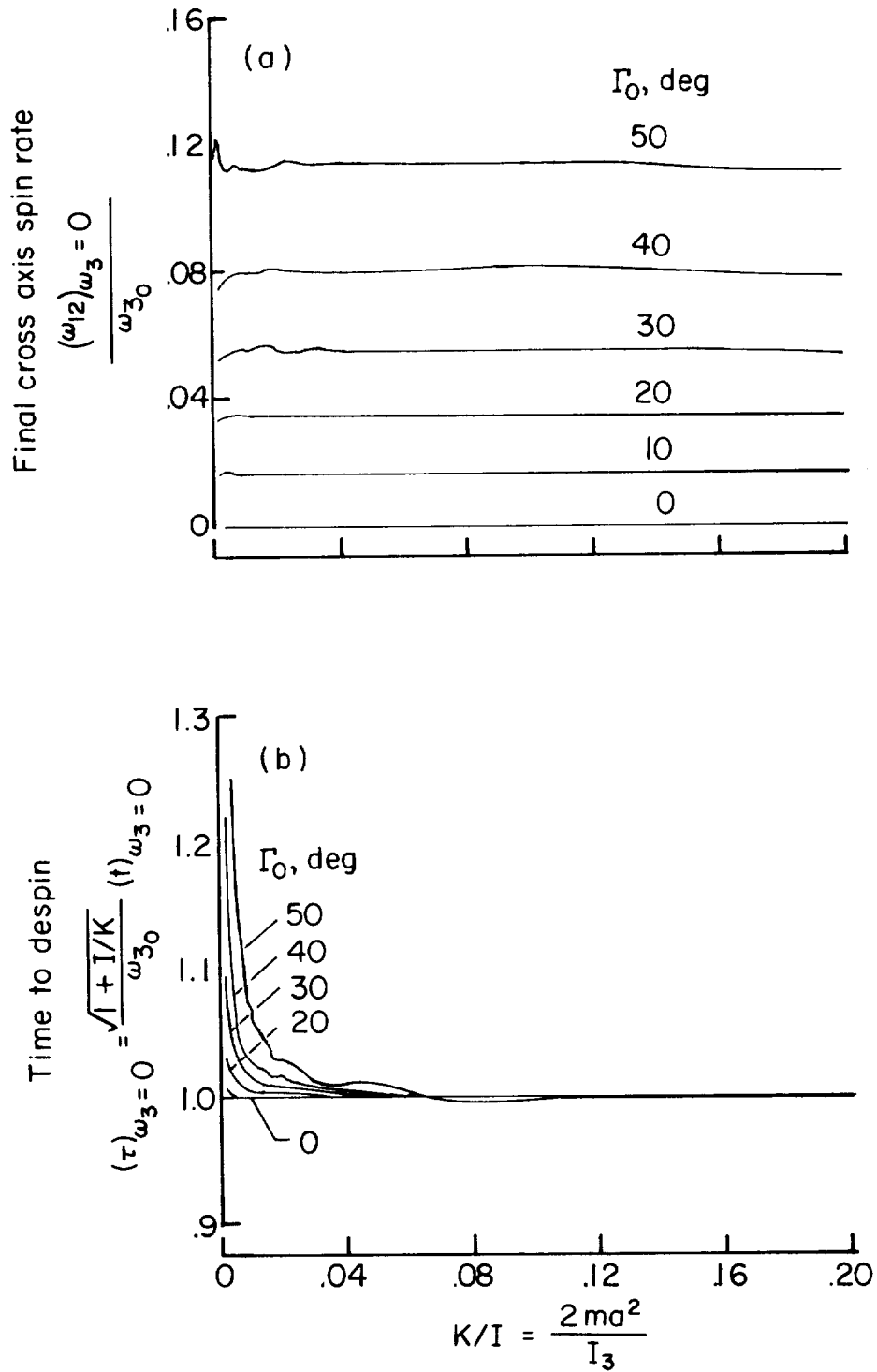


Figure 4.- Variation of significant nondimensional design parameters with ratio of inertia factors for different values of initial coning angle and for $I = 0.1$.

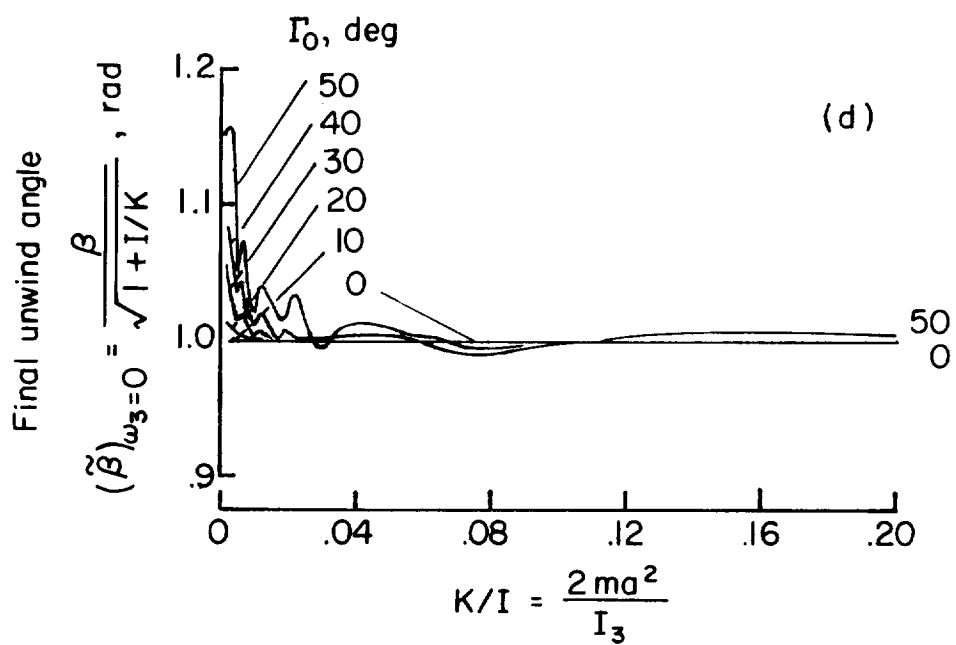
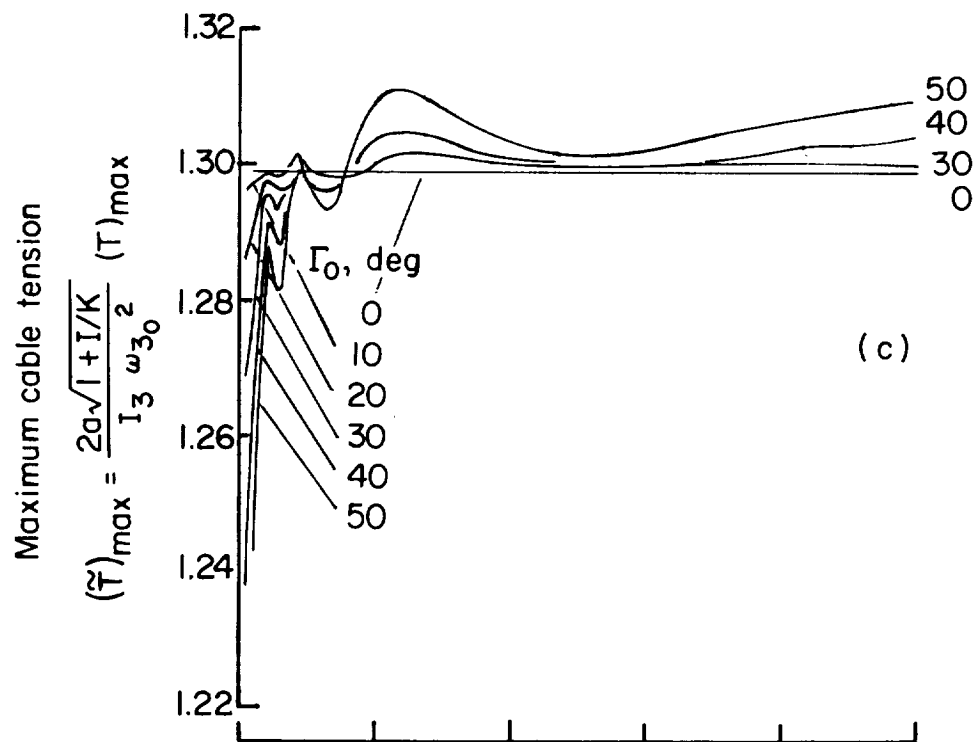


Figure 4.- Concluded.

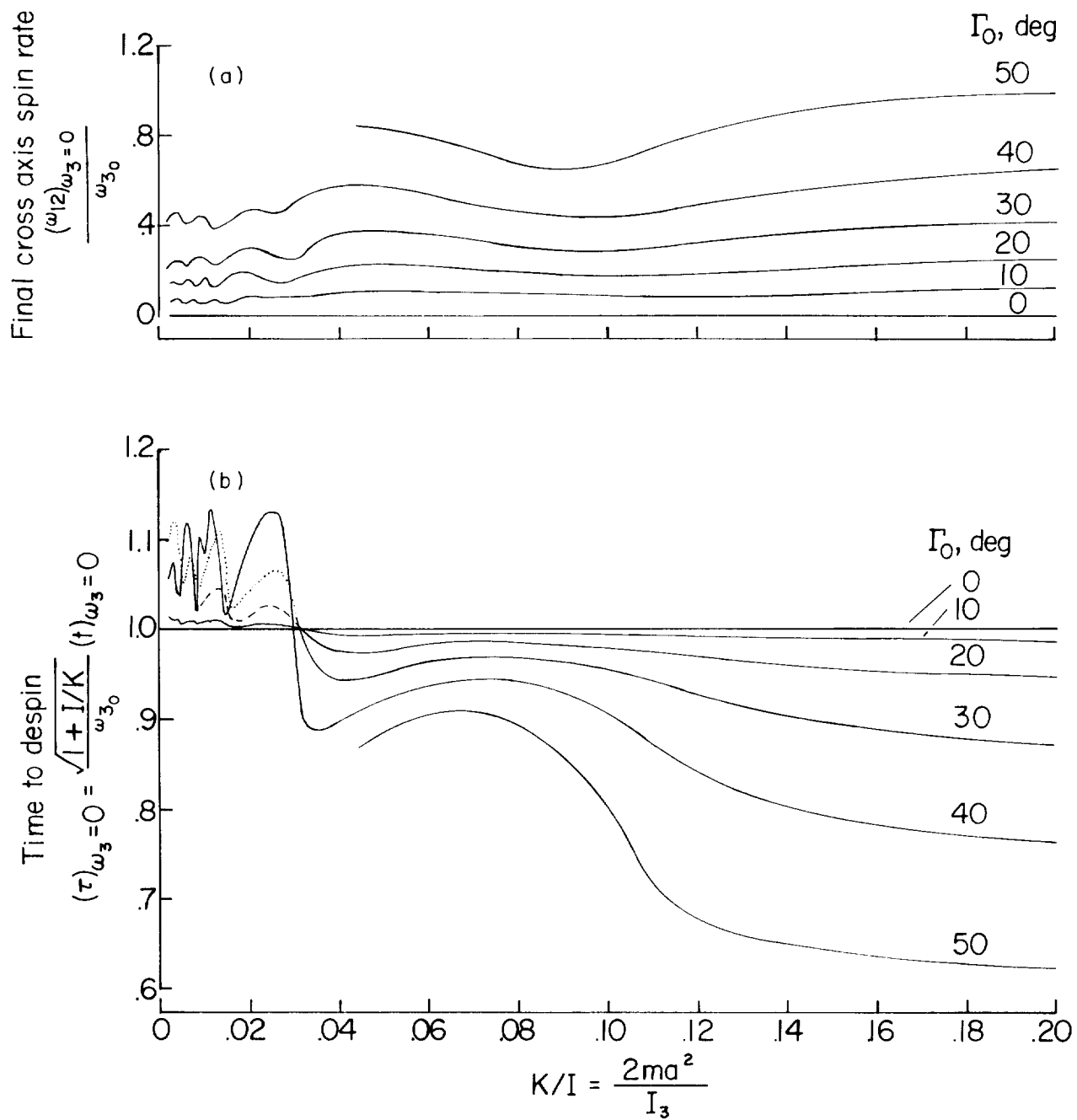


Figure 5.- Variation of significant nondimensional design parameters with ratio of inertia factors for different values of initial coning angle and for $I = 0.9$. Dashed and dotted curves are used only for clarity.

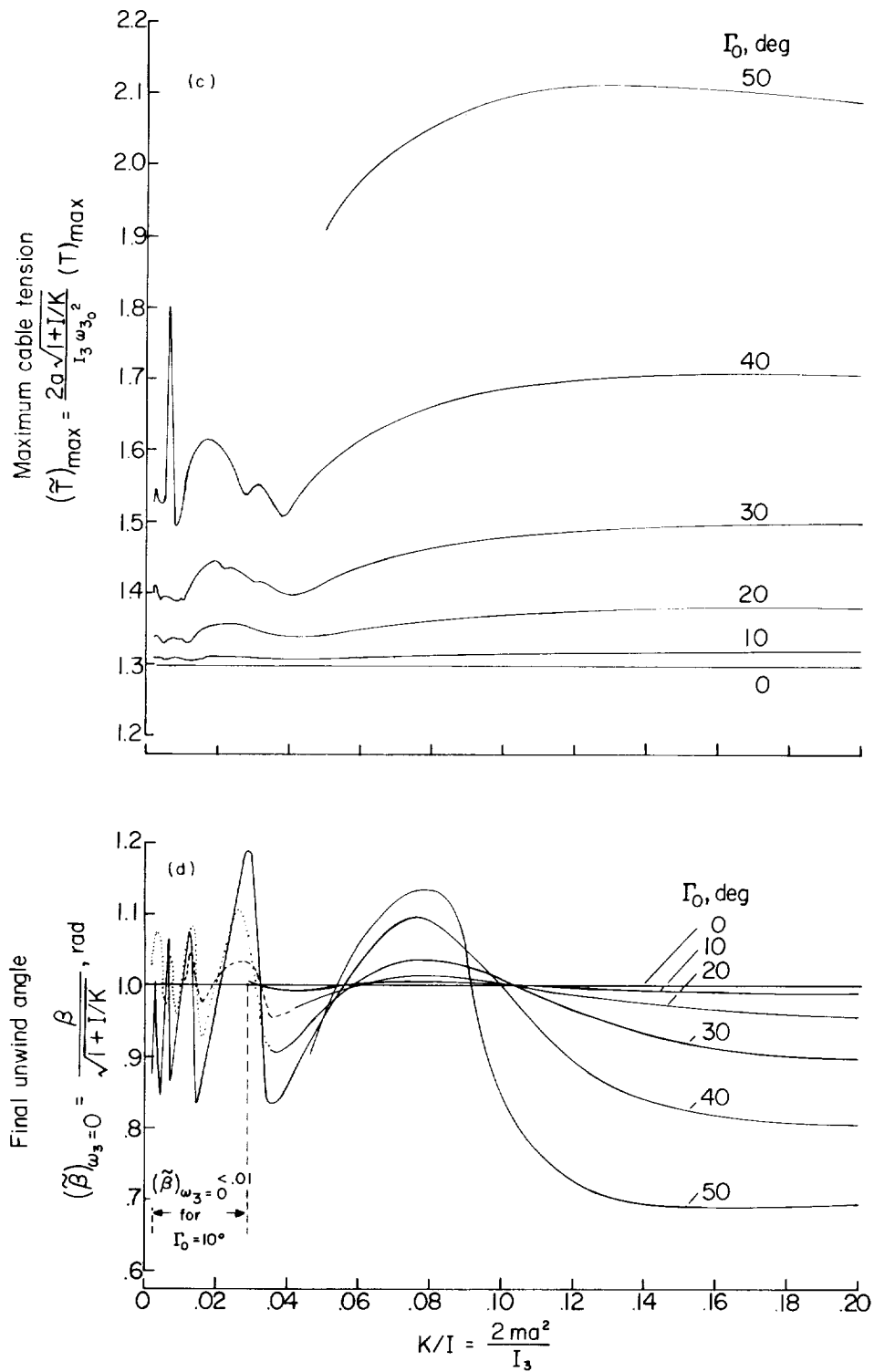


Figure 5.- Concluded.

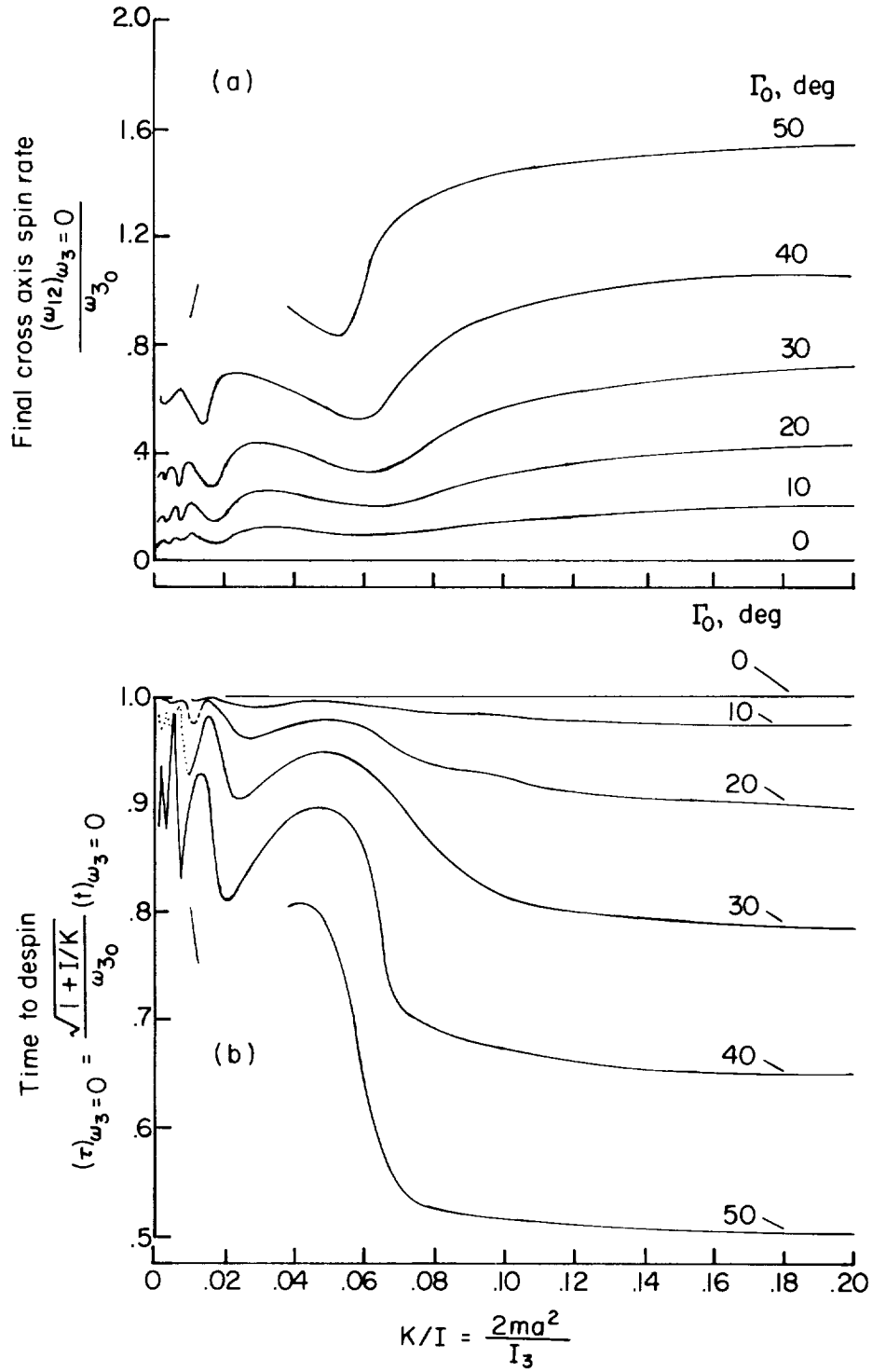


Figure 6.- Variation of significant nondimensional parameters with ratio of inertia factors for different values of initial coning angle and for $I = 1.3$. Dashed and dotted lines are used only for clarity.

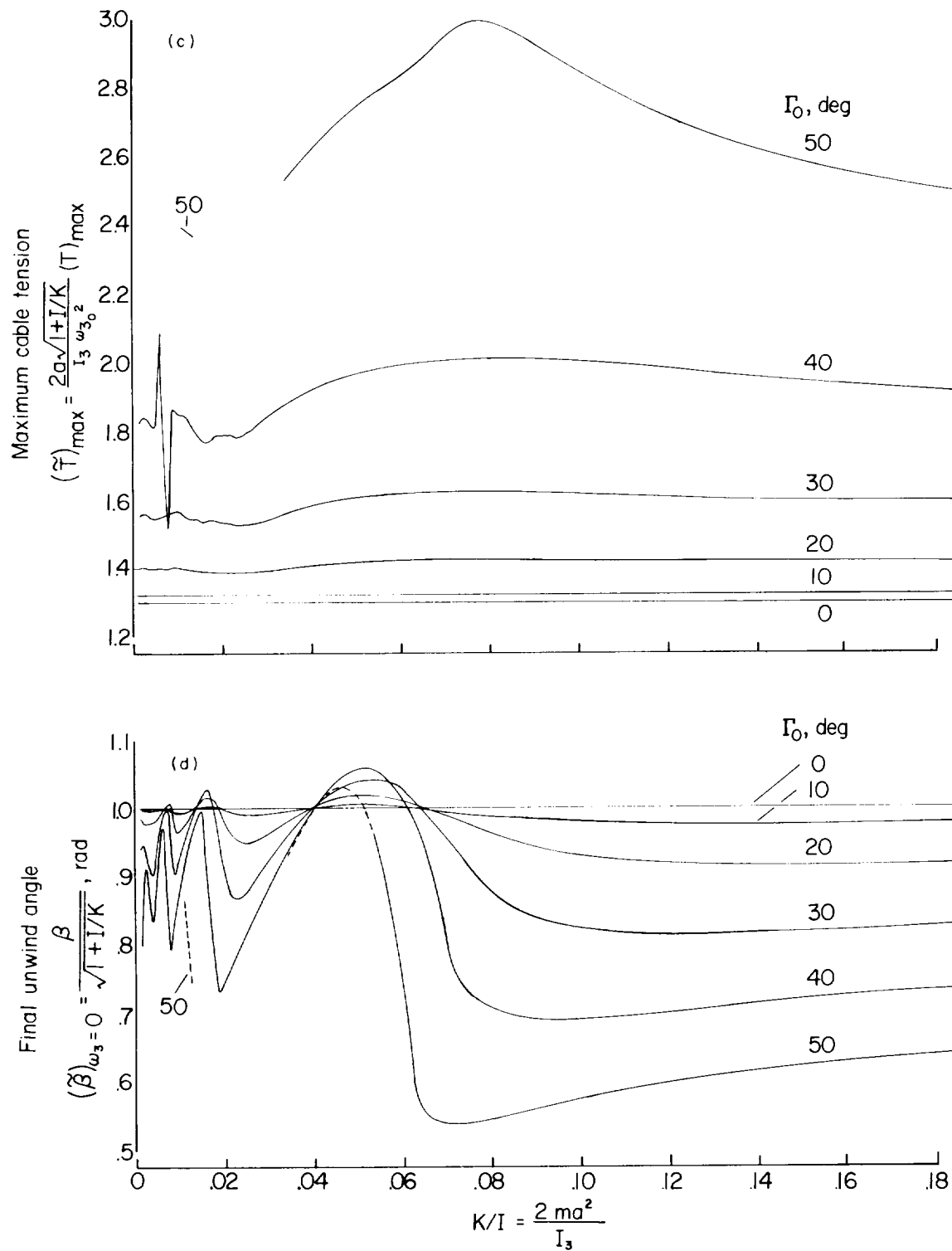


Figure 6.- Concluded.

